Research article

MRC

Received: 17 October 2013 Revised: 18 December 2013 Accepted: 20 December 2013 Published online in Wiley Online Library: 4 February 2014

(wileyonlinelibrary.com) DOI 10.1002/mrc.4044

Quantitative and qualitative ^{1}H, ^{13}C, and ^{15}N NMR spectroscopic investigation of the urea–formaldehyde resin synthesis

Oliver Steinhof,[a]* Éléonore J. Kibrik,[b] Günter Scherr[c] and Hans Hasse[b]

Urea–formaldehyde resins are bulk products of the chemical industry. Their synthesis involves a complex reaction network. The present work contributes to its elucidation by presenting results from detailed NMR spectroscopic studies with different methods. Besides ^{1}H NMR and ^{13}C NMR, ^{15}N NMR spectroscopy is also applied. ^{15}N-enriched urea was used for the investigations. A detailed NMR signal assignment and a model of the reaction network of the hydroxymethylation step of the synthesis are presented. Because of its higher spectral dispersion and the fact that all key reactions directly involve the nitrogen centers, ^{15}N NMR provides a much larger amount of detail than do ^{1}H and ^{13}C NMR spectroscopy. Symmetric and asymmetric dimethylol urea can be clearly distinguished and separated from monomethylol urea, trimethylol urea, and methylene-bridged urea. The existence of hemiformals of methylol urea is confirmed. 1,3,5-Oxadiazinan-4-on (uron) and its derivatives were not found in the reaction mixtures investigated here but were prepared via alternative routes. The molar ratios of formaldehyde to urea were 1, 2, and 4, the pH values 7.5 and 8.5, and the reaction temperature 60 °C.

Keywords: NMR; ^{1}H; ^{15}N; ^{13}C; urea–formaldehyde; quantitative NMR; virtual reference; 2D NMR; hydroxymethylation; adhesives

Introduction

Urea–formaldehyde (UF) resins are used as binders for wood products. The annual worldwide production was about $9.2 \cdot 10^6$ tons in 2003[1] and rose to $14.2 \cdot 10^6$ tons in 2006.[2] These resins are usually prepared in large-scale batch processes involving a pH-value step change. During the first phase, formaldehyde adds to urea under mildly alkaline conditions to form hydroxymethylated ureas.[3] In the second phase, these intermediates condensate under acidic conditions to form methylene-bridged and methoxymethylene-bridged ureas. The foundations to the understanding of this complex reaction network have been laid out by Kadowaki.[4] Later, Smythe,[5–7] Crowe and Lynch,[8,9] de Jong and de Jonge,[10–18] Landqvist,[19–28] and Kveton[29] reported on reaction pathways, reaction mechanisms, and reaction kinetics of the main components. Up to now, industrial processes for the production of UF resins are typically controlled by temperature and pH value. The degree of condensation is determined by macroscopic properties of the resin, usually viscosity or miscibility with water. There is practical knowledge available that enables relating these control parameters to product quality parameters like adhesiveness and activity. However, the molecular mechanisms responsible for the final properties of the product are not yet fully understood. The optimization of secondary performance properties of the UF resin like shelf life, hydrolytic stability, and formaldehyde emission[3] while keeping the aforementioned primary properties in the optimal range poses an additional challenge. Furthermore, low emission of formaldehyde from wood products is important. Significant reductions have been achieved,[30] but the final goal of zero formaldehyde emission still lies ahead. The UF reaction system is complex. This is due to the polydentate nature of urea as related to formaldehyde. The number of possible intermediates grows exponentially with the conversion rate after urea and formaldehyde are combined (Section on Chemical Reaction System). Further complexity arises from the formaldehyde–water reaction system[31–33] (Fig. 1), which is interconnected to the UF system via monomeric formaldehyde, being the reactive species in both systems. All reactions in the combined system are equilibrium reactions with rate constants varying by orders of magnitude. To gain analytical insight into the UF system, a noninvasive analytical technique is needed. NMR spectroscopy was chosen for the present study because of the wealth in structural information it provides, the possibility to quantify components directly, and the simplicity of the experimental setup. Combining ^{1}H, ^{13}C, and ^{15}N NMR spectroscopy with ^{15}N-enriched urea as starting material proved to be particularly useful. Already, the earliest NMR spectroscopic investigations of the UF system by Kambanis and Chiavarini reported on quantitative analysis with ^{1}H NMR spectroscopy.[34,35] Other early analyses of the system by ^{13}C NMR spectroscopy provide qualitative information only.[36–38] Tomita[39] reported the first quantitative analysis of finished resins by ^{13}C NMR spectroscopy, followed by Rammon *et al.*[40] and Kim.[41] Christjanson and Siimer combined ^{13}C NMR spectroscopy

* *Correspondence to: Oliver Steinhof, Institute of Thermodynamics and Thermal Process Engineering, Universität Stuttgart, 70569 Stuttgart, Germany. E-mail: steinhof@itt.uni-stuttgart.de*

a *Institute of Thermodynamics and Thermal Process Engineering, Universität Stuttgart, 70569 Stuttgart, Germany*

b *Laboratory of Engineering Thermodynamics, University of Kaiserslautern, 67663 Kaiserslautern, Germany*

c *BASF SE, 67056 Ludwigshafen, Germany*

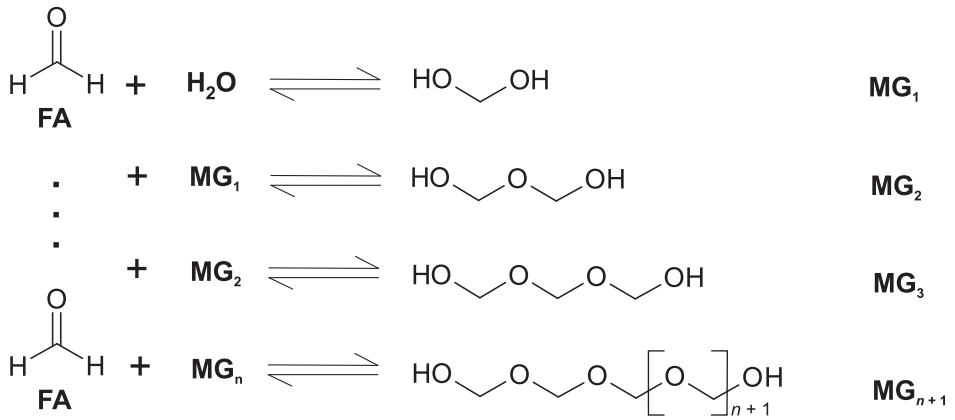

Figure 1. Chemical reactions in the formaldehyde–water system. Molecular formaldehyde CH_2O reacts with water to form oligomeric methylene glycols.

with thermal analysis.[42,43] Recently, Despres *et al.* [44] combined ^{13}C NMR spectroscopy with matrix-assisted laser desorption/ionization time of flight mass spectrometry to provide a detailed analysis of UF and melamine–UF resins. ^{15}N NMR spectroscopy was first used by Ebdon *et al.*[45,46] to characterize UF intermediates as well as freeze-dried resins, relying on ^{15}N in natural abundance. Acquisition times of several days were required to achieve an acceptable signal-to-noise ratio. Thomson[47] applied ^{15}N DEPT NMR spectroscopy to investigate the curing process of UF resins. The most recent work in this area has been reported by Angelatos[48] and Philbrook *et al.*,[49] who both used ^{15}N NMR correlation spectroscopy to identify possible copolymers between urea and melamine in melamine–UF resins. One of the authors studied the UF system with a combination of 1D and 2D NMR spectroscopy of ^{1}H, ^{13}C, and ^{15}N while making use of isotope-enriched urea.[50] In the present work, ^{15}N NMR spectroscopy was used to study the UF system not only qualitatively but also quantitatively. Furthermore, for the first time, ^{15}N-enriched urea was used to study this system. In combination with the results from other NMR spectroscopic methods, this gives a particularly rich and detailed picture of the complex chemistry of the studied system. The main parameters of the production process of UF resins are (1) molar ratio formaldehyde/urea (FA/U ratio) in the feed mixture, (2) water content of the feed mixture (specified here by the overall mass fraction of formaldehyde in the aqueous formaldehyde solution used to prepare the feed mixture), (3) temperature, and (4) pH value. Both temperature and pH value can be changed during the production process. Also time-dependent addition of reactants can be applied. It is not trivial to optimize a process of this kind with regard to a complex set of goals as discussed earlier. The present study was carried out in ranges of parameters 1–4, which cover industrially relevant conditions.[51] The FA/U ratio was studied at 1, 2, and 4 using an aqueous formaldehyde solution with a formaldehyde concentration of 0.3 g/g. This concentration was chosen because it is the highest one that can still be handled at ambient temperature without formation of precipitates. These experiments were carried out at pH values of 7.5 and 8.5, all at a temperature of 60 °C. While this temperature is lower than the temperatures encountered in most industrial UF resin processes, the observed line shapes in the NMR spectra are still sufficiently narrow to allow for acceptable peak assignment and quantitative analysis. It is not expected that the pH value has an influence on the equilibria of the individual reactions. However, it was found valuable to verify this influence.

Chemical Reaction System

Chemistry of the formaldehyde–water system

Formaldehyde is a gas at ambient conditions and commonly used as liquid, aqueous solutions. These solutions are highly reactive multicomponent mixtures.[33] In aqueous solutions, formaldehyde is mainly present as poly(oxymethylene)glycols or MG_n (Fig. 1). The amount of monomeric formaldehyde CH_2O is very low in these solutions and is expected to be below $1 \cdot 10^{-3}$ mol/mol for the conditions studied in the present work.[52,53] Hence, formaldehyde is predominantly present as methylene glycol MG_1 and its oligomers MG_n. The average chain length of the oligomers increases with increasing overall formaldehyde concentration. The reaction equilibria are only slightly temperature dependent. These reactions occur in all aqueous formaldehyde solutions and are subject to both acid and base catalyses. As formaldehyde is an important base chemical, these reactions have extensively been studied (Hahnenstein *et al.*,[31,54,55] Dahn and Pechy,[56] Maiwald *et al.*,[57,58] Kuhnert,[59] and the references therein). Both the equilibrium constants and reaction rates are well known. There are several possible side reactions in the formaldehyde–water system of which the Cannizzaro reaction, yielding formic acid and methanol, is the most important (Section on Side Reactions in the UF System).[60,61] Remaining from the production process and added as a stabilizer, aqueous formaldehyde solutions often also contain methanol. With methanol, formaldehyde forms the hemiformals of the oligomeric polyoxymethylene glycols. It exhibits a reaction scheme that is similar to that with water. As the formaldehyde solutions used in the present study contained only very small amounts of methanol, the reactions of formaldehyde with methanol play no role in the present study. Abundant data on the equilibria and kinetics of these reactions have been reported elsewhere (Ott *et al.*[62] and the references therein).

Main reactions in the UF system

The four basic reactions defining the chemistry of UF resins are described as follows:

1. *Addition of formaldehyde to urea,* leading to monomethylol urea (MMU). Formaldehyde can also add to the remaining

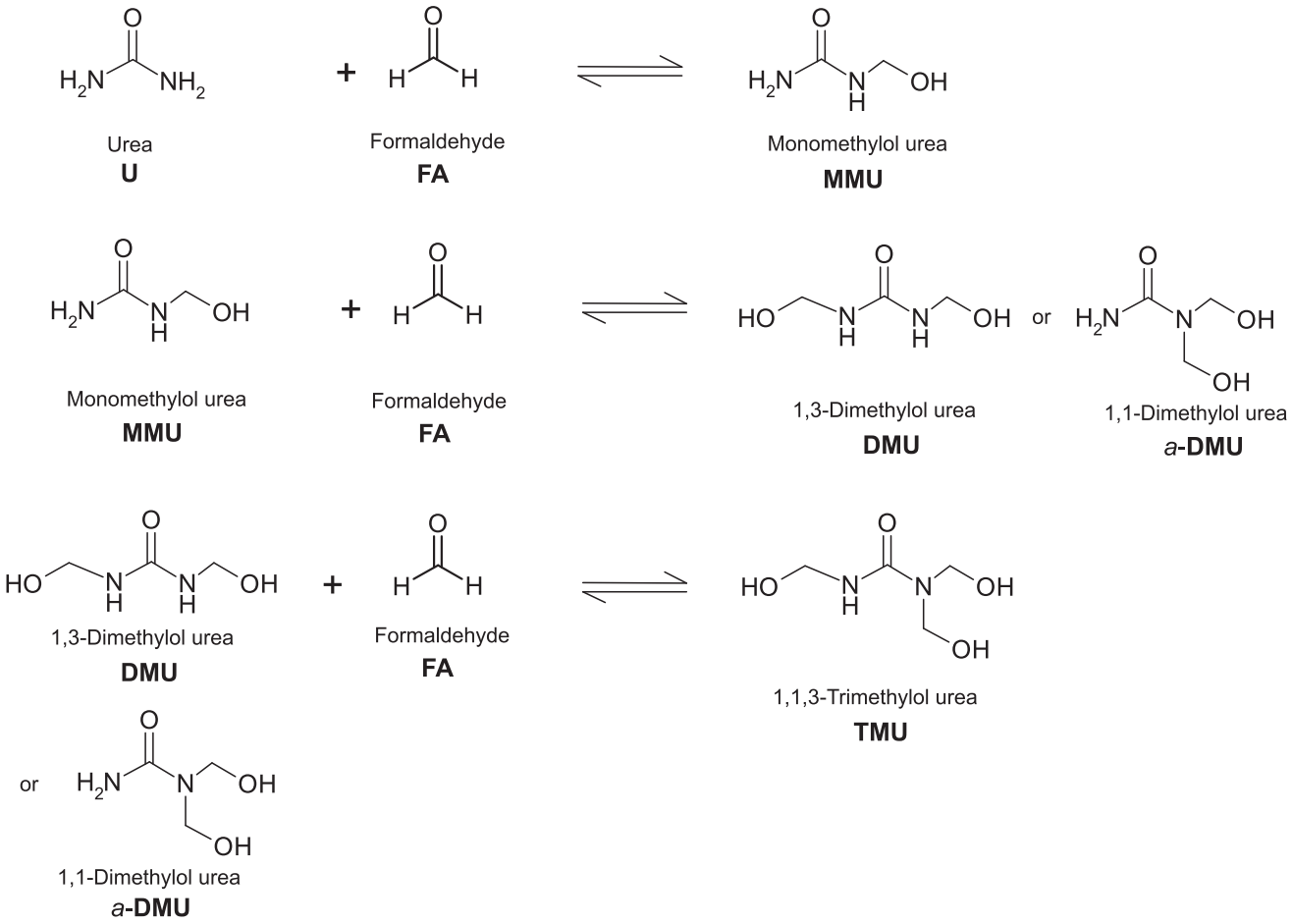

Figure 2. Hydroxymethylation of urea. Urea binds up to three molecules of formaldehyde.

amide protons of MMU, leading to dimethylol and trimethylol urea (TMU; Fig. 2). Substitution of all four amide protons has never been reported. This reaction follows general acid–base catalysis [63]. In industrial application, this conversion is carried out at a pH value between 7 and 9.

2. *Formation of hemiformals of hydroxymethyl groups.* Formaldehyde adds to existing hydroxymethyl groups to form oligomeric hemiformals (Fig. 3). This reaction is similar to the formation of methylene glycols in the formaldehyde–water system.
3. *Condensation of methylol ureas with urea* and other intermediates possessing amide protons, leading to methylene-bridged urea derivatives (Fig. 4). This reaction follows general acid catalysis. In most industrial processes, this is performed at pH values of 4–6. However, the reaction also proceeds at lower rates at pH values exceeding 6, as was shown in this work.
4. *Condensation of hydroxymethyl hemiformals with urea* or hydroxymethylated urea forming methoxymethylene or 'ether' bridges (Fig. 5). Recently, Kibrik *et al.*[64,65] provided evidence that these intermediates do exist in UF reaction mixtures. Literature is ambiguous on whether the formation of these components is favored under basic conditions during hydroxymethylation[13,66–71] or under neutral to acidic conditions during condensation and curing.[29,72–76] In this work, methoxymethylene bridges were not taken into account. The peak assignment was completed with the intermediates listed in Table 1.

Urea entities can connect via formation of methylene bridges and likely via methoxymethylene bridges. Because one urea unit can form at least three of these bridges, a polymer with a 3D network is formed during condensation in the final product. Starting with urea and formaldehyde, the number of possible intermediates grows exponentially while the conversion proceeds. All reactions are reversible, the presence of water provided. An overview of the reaction pathways in the UF reaction system is depicted in Fig. 6. All pathways shown were confirmed during the course of this work except for methoxymethylene-bridged diureas. Although strong indications suggest their existence,[64,65] literature does not report isolation or characterization of specific examples of these intermediates. The main pathway, temporary intermediates, and selected side reactions are indicated.

Side reactions in the UF system

Intramolecular condensation of symmetric dimethylol urea (DMU) and its derivatives leads to cyclic structures of the uron type. Isolation and identification of these structures in UF resins have been reported earlier by Kadowaki.[4] Their formation was reported to take place under both alkaline and acidic conditions. From that observation, it could be concluded that these species form not only during condensation but also during the hydroxymethy-

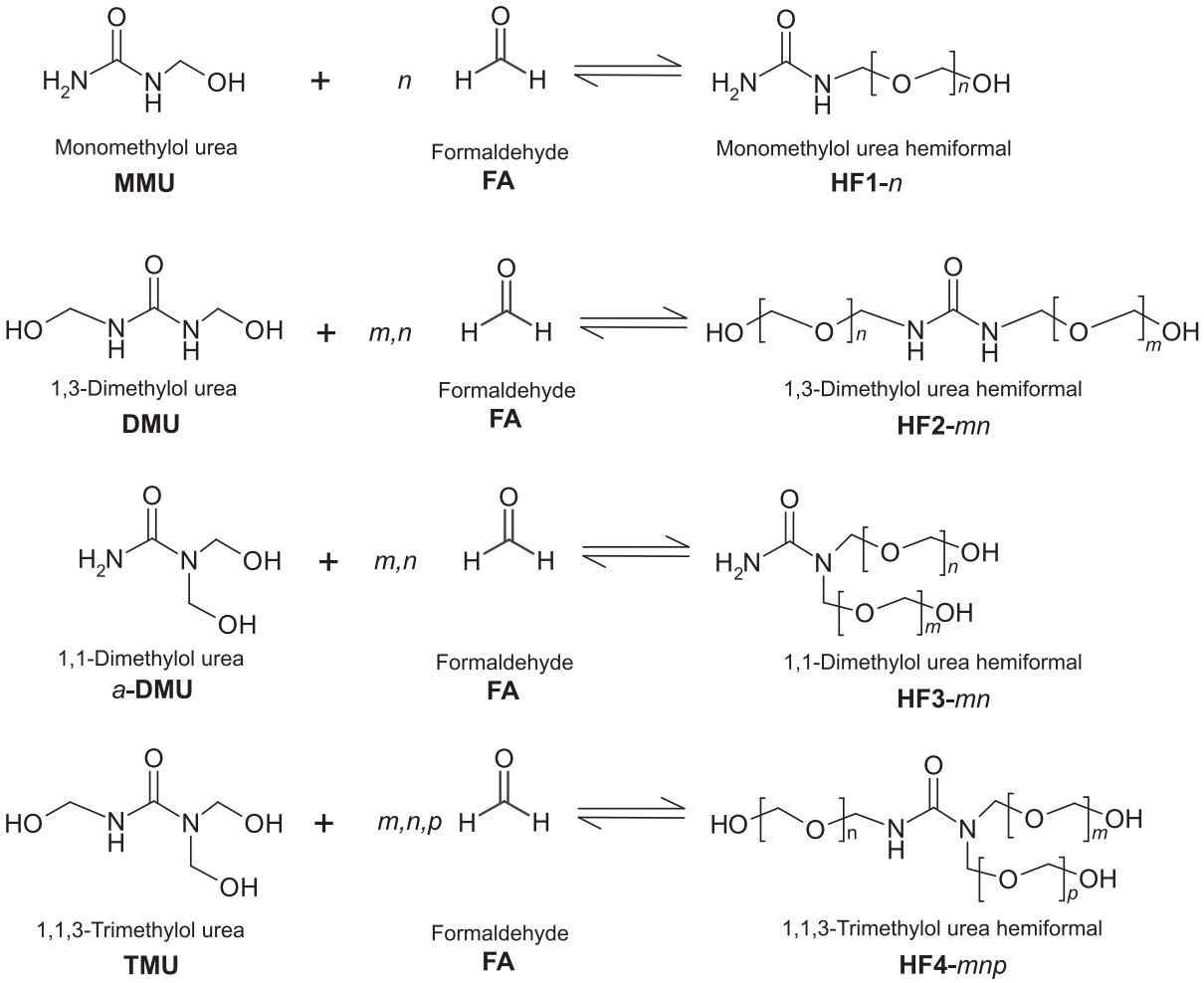

Figure 3. Overview of reactions of formaldehyde with the hydroxymethyl groups of monomethylol urea leading to different hemiformals.

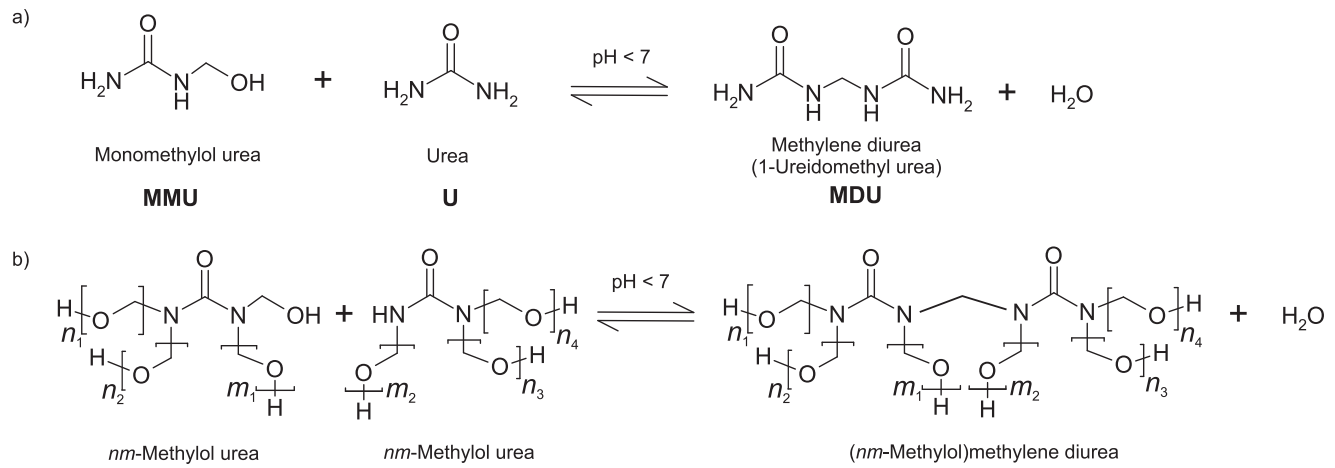

Figure 4. Condensation reactions in the urea–formaldehyde system, formation of methylene-bridged intermediates: (a) formation of methylene diurea; (b) general description of the condensation to methylene diureas.

lation step under basic conditions.[75,77,78] In the present study, formation of these cyclic structures during hydroxymethylation under conditions similar to the industrial process could not be confirmed. However, uron structures were prepared via alternative pathways and were characterized successfully. Under acidic conditions, methanol and other alcohols are converted to ethers. In case of methanol, methoxymethylene ethers are formed from hydroxymethyl groups. This reduces the potential of the resin to

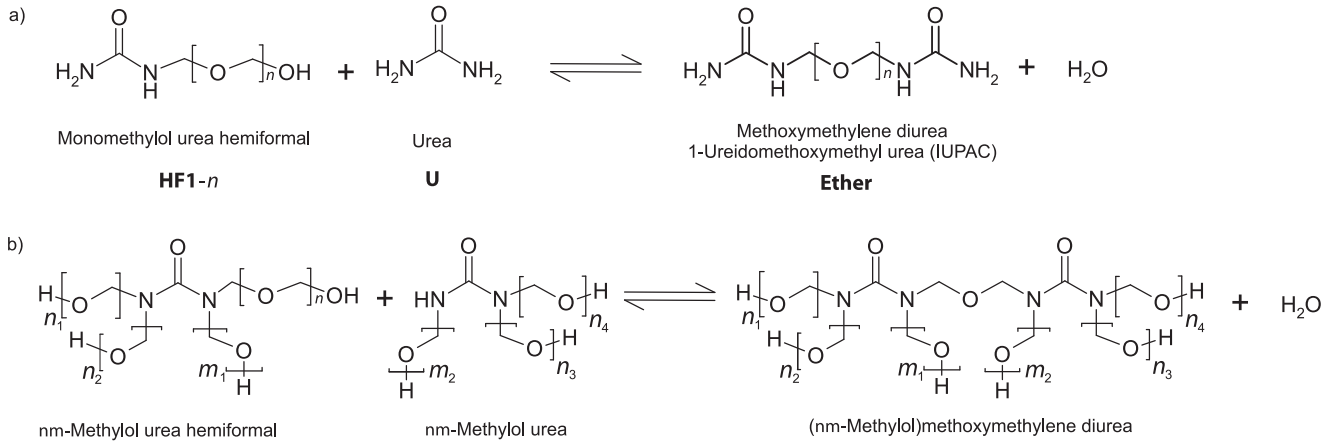

Figure 5. Condensation reactions in the urea–formaldehyde system and formation of ether-bridged intermediates: (a) formation of methoxymethylene diurea from hemiformal HF1-*n* and urea; (b) general description of the condensation to methoxymethylene diurea.

Table 1. Synthesized and characterized urea–formaldehyde intermediates

Component	Abbreviation
Monomethylol urea	MMU
1,3-Dimethylol urea	DMU
1-Ureidomethyl urea	MDU
1-Hydroxymethyl-3-(3-hydroxymethylureidomethyl) urea	DM-MDU
1,3-Bis-methoxymethyl urea	—
1,3,5-Oxadiazinan-4-on	Uron
3-Hydroxymethyl-1,3,5-oxadiazinan-4-on	Hydroxymethyl uron
3,5-Bis-hydroxymethyl-1,3,5-oxadiazinan-4-on	Bishydroxymethyl uron

form cross-links due to blockage of required functional groups. This results in a reduced activity of the resin, which is synonymous with lower product quality.[3] Hence, formaldehyde solutions with low methanol content are preferred as feed material for commercial production. Dissociation of urea leads to the formation of ammonia,[79] which reacts with formaldehyde to urotropine. Because of the slow dissociation rate of urea compared to the hydroxymethylation reaction under the studied conditions, only traces of this component were identified in the present study.[50]

Experiments

Approach

A stepwise approach was taken toward peak assignment. At first, selected intermediates were synthesized and characterized by ^{1}H, ^{13}C, and ^{15}N NMR spectroscopy to establish a basic peak assignment. Table 1 lists the components that were prepared and characterized for this purpose. Details on their preparation are described in the Synthesis of Single Components section in the Appendix. In a second step, mixtures of urea and formaldehyde were prepared with ^{15}N-enriched urea (Section on Sample Preparation and Analysis) and analyzed by 1D directly detected ^{1}H, ^{13}C, and ^{15}N NMR spectroscopy (Sections on NMR Spectroscopy and Peak Assignment). Directly detected 1D NMR spectroscopy was chosen here for its speed and robustness. It is capable of detecting tertiary nitrogen and carbon centers directly while maintaining good resolution and minimal artifacts. Table 2 lists the composition and the experimental conditions of the analyzed reaction mixtures. In a third step, the ^{15}N and ^{13}C NMR spectra of the reaction mixtures were analyzed qualitatively to refine signal assignment (Sections on ^{1}H NMR Spectra, ^{13}C NMR Spectra, and ^{15}N NMR Spectra). Comparing the spectra of mixtures of different FA/U ratios at different pH values proved to be essential for peak assignment. As a fourth step, this was followed by quantitative analysis (Sections on Quantitative Analysis of 1D ^{15}N NMR Spectra and Quantitative Analysis of 1D ^{13}C NMR Spectra). Selected samples were also studied by 2D NMR spectroscopy.

Materials

Urea in prills of ≥99% purity was supplied by BASF SE (Ludwigshafen, Germany). ^{15}N-labeled urea, enriched to 98% in ^{15}N, was purchased from Deutero GmbH (Kastellaun, Germany). Both materials were used without further purification. Aqueous formaldehyde solution with a formaldehyde mass fraction of 0.3 g/g and a methanol mass fraction of less than 0.01 g/g was supplied by BASF SE (Ludwigshafen, Germany). Before use, the formaldehyde concentration was determined titrimetrically. The pH value was adjusted with an aqueous solution of sodium hydroxide (0.1 g/g) directly before use. An aqueous phosphate buffer of the concentration of 1 or 0.1 mol/l was added as required. All other reagents and solvents were obtained from commercial sources with a minimum purity of 99% and used without further purification.

NMR spectroscopy

All spectra were recorded on a Varian Unity Inova 400 spectrometer (Varian, Palo Alto, USA) with a field strength of 9.4 T. As all measurements were conducted in aqueous solution, the chemical shifts of ^{1}H and ^{13}C were referenced to the water-soluble internal standard 2,2-dimethyl-2-silapentan-5-sulfonic acid sodium salt $(CH_3)_3\,Si\,(CH_2)_3\,SO_3Na$.[80] For the 1D spectra, simple 1D experiments were used. Both the ^{15}N and ^{13}C pulse sequences supported decoupling. For each ^{1}H NMR spectrum, only one transient was recorded. The chemical shifts in the ^{15}N domain were referenced to CH_3NO_2, which was used as an external standard. Because of sensitivity and solubility issues, $^{15}NH_4{}^{15}NO_3$ was added

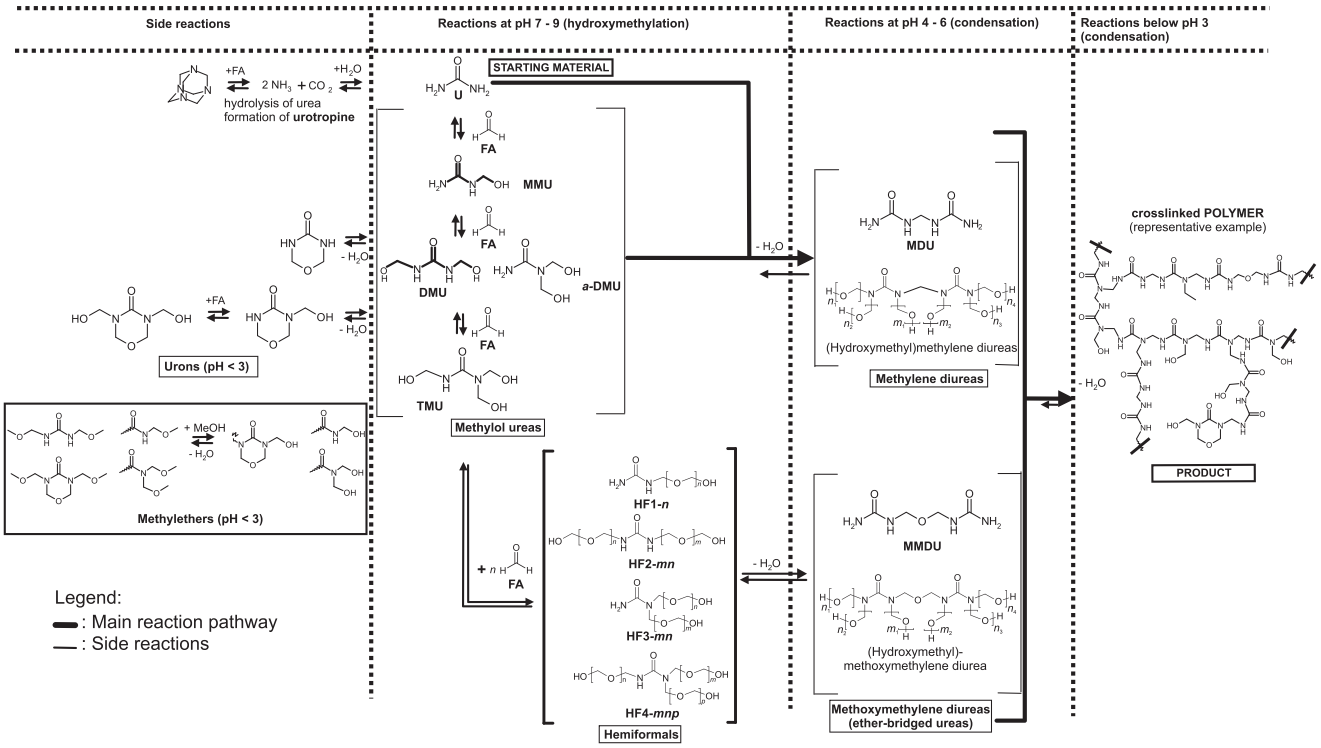

Figure 6. Overview of urea–formaldehyde reaction network. The main reaction pathways are indicated in bold.

Table 2. Composition and reaction conditions of the reaction mixtures analyzed in this work

Sample no.	FA/U ratio (mol/mol)	pH value	Buffer concentration (mol/l)	x_i Formaldehyde	Urea	Water
1	1	7.5	1.0	0.059	0.059	0.881
2	2	7.5	1.0	0.140	0.070	0.789
3	4	7.5	1.0	0.115	0.029	0.855
4	1	8.5	1.0	0.059	0.059	0.881
5	1	8.5	0.1	0.059	0.059	0.881
6	2	8.5	1.0	0.140	0.070	0.789
7	4	8.5	1.0	0.115	0.029	0.855

as an internal secondary standard to the mixtures (the resonance of $^{15}NO_3$ was used as a reference). The acquisition parameters for 1D ^{15}N NMR spectra were chosen with regard to the longitudinal relaxation times T_1 of the nitrogen centers. The T_1 times for the NH_2 and NHR groups (R = CH_2—OH, CH_2X) were found to be in the range of 1–5 s using standard experiments.[81] For the tertiary NR_2 groups, T_1 was found to be between 28 and 54 s. The pulse angle was set to 45°, where complete relaxation has taken place after $0.5 \cdot T_1$.[81] The time between scans was set to 60 s. Hence, even the tertiary nitrogen centers relax almost completely. See Malz[82,83] and Maiwald[84–86] for further information on quantitative NMR spectroscopy. Inverse gated proton decoupling was applied to achieve a sufficient signal-to-noise ratio. Acquisition time was 3 s, and the spectral window was 25 kHz. The data were acquired at a digital resolution of 0.16 Hz per data point. Five transients were recorded at an FA/U ratio of 1, while nine transients were recorded at FA/U ratios of 2 and 4 for sensitivity reasons. So the total acquisition time for a 1D ^{15}N NMR spectrum amounted to 5–10 min. For the ^{13}C spectra, 64 or 128 transients were recorded at a pulse angle of 56.8° with 15-s relaxation time and inverse gated proton decoupling. All ^{13}C shifts reported here are corrected by −2.66 ppm to be in line with shifts referenced to TMS.[87] The applied ^{15}N pulse sequence additionally supported a virtual reference (VR) signal, which was used in this study to relate signal integrals to actual analyte concentrations in the sample. The method was pioneered by Mahon[88] and is also known as Electronic REference To access In vivo Concentrations (ERETIC).[84,89,90] A synthetic FID is generated by the NMR console via an additional channel and injected into the probe during acquisition. The Transistor Transistor Logic (TTL) signal from the console was attenuated by 75 dB using manual step attenuators. The resulting synthetic signal is referenced to a solution of a standard component of known concentration. Later, the signal can be used as a reference to quantify analyte signals in other samples. The technique relies on the excellent stability of modern spectrometers. Hence, it is important that all instrument parameters remain and also that the magnetic susceptibility remain unchanged between the analyses of the reference sample and the

sample in question. In this study, the VR was referenced against an aqueous solution of ^{15}N-enriched urea of known concentration. It was used here to determine the actual molar amounts of UF intermediates in the reaction mixtures. This information was used also to determine the recovery rate of urea in these reaction mixtures (Supporting Information). VR was applied to ^{15}N NMR spectroscopy only.

Sample preparation and analysis

The same procedure was used for all samples. All experiments were conducted directly in standard 5-mm NMR tubes. Table 2 gives an overview of the samples studied. First, solid urea was dissolved in phosphate buffer of the required pH value in the NMR tube. Then, the secondary reference standard $^{15}NH_4{}^{15}NO_3$ (^{15}N in 99% abundance, 0.01 g/g with regard to urea) was added, followed by the aqueous formaldehyde solution (0.3 g/g). Directly before use, the pH value of the formaldehyde solution was adjusted using an aqueous solution of sodium hydroxide. The sample was mixed and equilibrated for 45 min in a thermal bath of 60 °C before being transferred to the NMR spectrometer. The variation in the FA/U ratio was achieved by changing the quantities of formaldehyde and urea. Phosphate buffer was used to stabilize the pH value and to maintain a sufficient and uniform fill level of the NMR tubes. Hence, the water concentration was not controlled; water was always present in large excess. The buffer solution had a buffer salt concentration of 1 mol/l for all samples

Table 3. Formaldehyde–urea intermediates: number of signals j in the ^{15}N NMR spectrum of component i consisting of peaks A_{ij} (in case of MG_1 to MG_3, this refers to the peaks in the ^{13}C NMR spectrum), stoichiometric factors z_i, number of urea units g_i, and number of formaldehyde units f_i for the analyzed components

Intermediate	Abbreviation	j	z_i	g_i	f_i
Urea	U	1	2	1	0
Monomethylol urea	MMU	2	2	1	1
1,3-Dimethylol urea	DMU	1	2	1	2
1,1-Dimethylol urea	*a*-DMU	2	2	1	2
Trimethylol urea	TMU	2	2	1	3
Monomethylol urea hemiformal	HF1-*n*	2	2	1	2
1,3-Dimethylol urea hemiformals	HF2-0*n*	1…*n*	2	1	3
1,3-Dimethylol urea hemiformals	HF2-*mn*	1…*n*	2	1	4
1,1-Dimethylol urea hemiformals	HF3-0*n*	2…*n*	2	1	3
Trimethylol urea hemiformals	HF4-0*np*	2…*n*	2	1	4
Trimethylol urea hemiformals	HF4-*mn*0	2…*n*	2	1	4
1-Ureidomethyl urea, Methylene diurea	MDU	2	4	2	1
1-Ureidomethyl ureas, Methylene diureas	MDUs	3…*n*	4	2	2
Methoxymethylene diureas	Ether	2…*n*	4	2	2
Methylene glycol	MG_1	1	1	0	1
Dimethylene glycol	MG_2	1	2	0	2
Trimethylene glycol	MG_3	2	2 + 1	0	3

Table 4. Component NMR chemical shifts, part I: urea and monomethylol ureas

			Functional group (chemical shift/ppm)					
Component, CAS no.	Formula, name	Nucleus	C=O	NH_2	$NHCH_2OH$	$NH(CH_2OH)_2$	$NHCH_2NR$	HFn-***mnp***
U [57-13-6]	CH_4N_2O Urea	^{1}H	—	5.7	—	—	—	—
		^{13}C	162.5	—	—	—	—	—
		^{15}N	—	−303.7	—	—	—	—
MMU [1000-82-4]	$C_2H_6N_2O_2$ Monomethylol urea	^{1}H	—	5.8	6.95; **4.64**	—	—	—
		^{13}C	160.8	—	64.3	—	—	—
		^{15}N	—	−304.8	−280.7	—	—	—
DMU [140-95-4]	$C_3H_8N_2O_3$ 1,3-Dimethylol urea	^{1}H	—	—	6.95; **4.69**	—	—	—
		^{13}C	159.3	—	64.4	—	—	—
		^{15}N	—	—	−280.5	—	—	—
a-DMU [1448-99-3]	$C_3H_8N_2O_3$ 1,1-Dimethylol urea	^{1}H	—	6.05	—	—	—	—
		^{13}C	160.2	—	70.8	—	—	—
		^{15}N	—	−302.8	−257.5	—	—	—
TMU [13329-70-9]	$C_4H_{10}N_2O_4$ Trimethylol urea	^{1}H	—	—	7.3	—	—	—
		^{13}C	158.8	—	64.6	71	—	—
		^{15}N	—	—	−279	−258	—	—

Table 5. Component NMR chemical shifts, part IIa: hemiformals of monomethylol ureas

			Functional group (chemical shift/ppm)					
Component, CAS no.	Formula, name	Nucleus	C=O	NH_2	NHC**H**$_2$OH	NH(CH_2OH)$_2$	NHC**H**$_2$NR	HFn-***mnp***
HF1-*n* *n*= 1	$C_2H_6N_2O_2 + n \cdot CH_2O$ Monomethylol urea hemiformal	^{1}H	—	5.8	—	—	—	—
		^{13}C	160.8	—	—	—	—	—
		^{15}N	—	−303.4	—	—	—	—
HF2-0*n* *n* = 1, *m* = 0	$C_3H_8N_2O_3 + n \cdot CH_2O$ 1,3-Dimethylol urea hemiformal	^{1}H	—	—	6.95	—	—	7.05
		^{13}C	159.3	—	64.5	—	—	68.6; **86.0–86.5**
		^{15}N	—	—	−279.5	—	—	−285.2
HF2-*mn* *m*, *n* = 1	$C_3H_8N_2O_3 + m \cdot CH_2O + n \cdot CH_2O$ 1,3-Dimethylol urea hemiformals	^{1}H	—	—	—	—	—	7.05
		^{13}C	159.3	—	—	—	—	68.6; **86.0–86.5**
		^{15}N	—	—	—	—	—	−284.9

Table 6. Component NMR chemical shifts, part IIb: hemiformals of monomethylol urea

			Functional group (chemical shift/ppm)					
component, CAS no.	Formula, name	Nucleus	C=O	NH_2	NHC**H**$_2$OH	NH(CH_2OH)$_2$	NHC**H**$_2$NR	HFn-***mnp***
HF3-*mn* *m*, *n* = 1	$C_3H_8N_2O_3 + m \cdot CH_2O + n \cdot CH_2O$ 1,1-Dimethylol urea hemiformals	^{1}H	—	6.1	—	—	—	—
		^{13}C	160.2	—	—	—	—	75.0; **86.0–86.5**
		^{15}N	—	−302.3	—	—	—	−269.8
HF4-0*n*0 *n* = 1, *m*, *p* = 0	$C_4H_{10}N_2O_4 + n \cdot CH_2O$ Trimethylol urea hemiformal	^{1}H	—	—	—	—	—	7.3
		^{13}C	158.8	—	—	71	—	68.6; **86.0–86.5**
		^{15}N	—	—	—	−257.5	—	−284.2
HF4-00*p* *p* = 1, *m*, *n* = 0	$C_4H_{10}N_2O_4 + p \cdot CH_2O$ Trimethylol urea hemiformal	^{1}H	—	—	7.3	—	—	—
		^{13}C	158.8	—	64.5	71	—	75.0; **86.0–86.5**
		^{15}N	—	—	−278.5	−264	—	−264

Table 7. Component NMR chemical shifts, part III: condensation products

			Functional group (chemical shift/ppm)					
Component, CAS no.	Formula, name	Nucleus	C=O	NH_2	NHC**H**$_2$OH	NH(CH_2OH)$_2$	NHC**H**$_2$NR	HFn-***mnp***
MDU [105214-18-4]	$C_3H_8N_4O_2$ Methylene diurea	^{1}H	—	5.8	—	—	6.8	—
		^{13}C	161.2	—	—	—	46.4	—
		^{15}N	—	−303.4	—	—	−285.5	—
MDUs	$C_3H_8N_4O_2$ $[CH_2O]_{m+n}$ *m* = 1 . . . 2, *n* = 1 . . . 4 Methylene diureas	^{1}H	—	5.8–6.0	7.1–7.3; 7.5	—	6.95–7.05	7.1–7.3
		^{13}C	160.8–158.8	—	64.1–64.4	71	46.3 (R=H); 52.8 (R=CH_2X)	68.5–69.5 (sec); 74.8–76.0 (tert); **86**
		^{15}N	—	−304.8	−280 to −279	−258	−286 to −284	−286.5 to −284.0; −270 to −269; −264 to −263
Ether [77214-83-6]	$C_4H_{10}N_4O_3$ Methoxymethylene diurea	^{1}H	—	—	—	—	—	—
		^{13}C	—	—	—	—	—	—
		^{15}N	—	—	—	—	—	—
Ethers	$C_4H_{10}N_4O_3$ $[CH_2O]_{m+n}$ *m* = 1 . . . 2, *n* = 1 . . . 4 Methoxymethylene diureas	^{1}H	—	—	—	—	—	—
		^{13}C	—	—	—	—	—	—
		^{15}N	—	—	—	—	—	—

Table 8. Component chemical shifts, part IV: methoxylated intermediates and urons

Component, CAS no.	Formula	Nucleus	Functional group (chemical shift/ppm) C=O	NH_2	$NHCH_2OH$	$NH(CH_2OH)_2$	$NHCH_2NR$	HFn-***mnp***
1,3-Bis-methoxymethyl urea [141-07-01]	$C_5H_{12}N_2O_3$	^1H	—	—	7.3; 4.58; 3.29 (OCH_3)	—	—	—
		^{13}C	159.5	—	72.1; 54.4 (OCH_3)	—	—	—
		^{15}N	—	—	−286.8	—	—	—
Uron [542-29-0]	$C_3H_6N_2O_2$ 1,3,5-Oxadiazinan-4-on	^1H	—	—	7.0; 4.86 (ring)	—	—	—
		^{13}C	156.5	—	74.1 (ring)	—	—	—
		^{15}N	—	—	—	—	—	—
Hydroxymethyl uron [22939-30-6]	$C_4H_8N_2O_3$	^1H	—	—	7.0; 4.81	4.99; 4.88 (ring)	—	—
		^{13}C	155.5	—	67.3	77.7; 74.6 (ring)	—	—
		^{15}N	—	—	—	—	—	—
Bis-hydroxymethyl uron [7327-69-7]	$C_5H_{10}N_2O_4$	^1H	—	—	4.84	5.02 (ring)	—	—
		^{13}C	154.8	—	67.7	78.2 (ring)	—	—
		^{15}N	—	—	—	—	—	—
Bis-methoxymethyl uron [7388-44-5]	$C_7H_{14}N_2O_4$	^1H	—	—	5.03; 3.34 (OCH_3)	4.78 (ring)	—	—
		^{13}C	155.1	—	78.3; 55.2 (OCH_3)	75.6 (ring)	—	—
		^{15}N	—	—	−280	—	—	—

Table 9. Component NMR chemical shifts, part V: formaldehyde. methylene glycols and other components

Component , CAS no.	Formula	Nucleus	Functional group (chemical shift/ppm) C=O	NH_2	$NHCH_2OH$	$NH(CH_2OH)_2$	$NHCH_2NR$	HFn-***mnp***
Formaldehyde [50-00-0]	CH_2O	^1H	—	—	—	—	—	—
		^{13}C	—	—	—	—	—	—
MG_1 [463-57-0]	CH_4O_2 Methylene glycol	^1H	—	—	**4.8 (OCH_2O)**	—	—	—
		^{13}C	—	—	82.4 (OCH_2O)	—	—	—
MG_2 [4407-89-0]	$C_2H_6O_3$	^1H	—	—	**4.85 (OCH_2O)**	—	—	—
		^{13}C	—	—	85.9 (OCH_2O)	—	—	—
MG_3 [3754-41-4]	$C_3H_8O_4$	^1H	—	—	**4.90**; **4.84 (OCH_2O)**	—	—	—
		^{13}C	—	—	89.8; 86.1 (OCH_2O)	—	—	—
$MG_{4...10}$	$CH_4O_2[CH_2O]_n$ ($n = 4...10$)	^1H	—	—	∼ **4.9**; ∼ **4.85 (OCH_2O)**	—	—	—
		^{13}C	—	—	∼90; ∼86 (OCH_2O)	—	—	—
Formic acid [64-18-6]	CH_2O_2	^1H	8.27	—	—	—	—	—
		^{13}C	165.9	—	—	—	—	—
Methylformiate [107-31-3]	$C_2H_4O_2$	^1H	8.18	—	3.8 (CH_3)	—	—	—
		^{13}C	164.5	—	51.5 (CH_3)	—	—	—
Urotropine [100-97-0]	$C_6H_{12}N_4$	^1H	—	—	—	—	4.64	—
		^{13}C	—	—	—	—	71.5	—
		^{15}N	—	—	—	—	−339.3	—
Methanol [67-56-1]	CH_4O	^1H	—	—	3.3 (CH_3)	—	—	—
		^{13}C	—	—	49.0 (CH_3)	—	—	—
Trioxane [110-88-3]	$C_3H_6O_3$	^1H	—	—	**5.2 (OCH_2O)**	—	—	—
		^{13}C	—	—	93.5 (OCH_2O)	—	—	—

except for sample 5, where it was 0.1 mol/l. Sample 5 is identical to sample 4 except for the lower concentration of the buffer solution used. The intention was to assess the influence of the buffer concentration on the sample composition. In the NMR spectrometer, the sample was maintained at 60 °C during acquisition. A ^{1}H NMR spectrum was acquired, followed by ^{15}N, ^{13}C, and in some cases, 2D NMR spectroscopy. Note that spectra were acquired after the reaction mixtures had reached equilibrium with regard to the hydroxymethylation reactions and to hemiformal formation (Figs 2 and 3). No equilibrium is attained with regard to the condensation reactions (Fig. 4). Under the reaction conditions investigated here, the reaction rates of the condensation reactions are distinctly smaller than (1) the reaction rates of the hydroxymethylation reaction, (2) the formation of hemiformals,[31,50,53] and (3) the time required for analysis of the reaction mixture. Hence, the condition of the reaction mixture is considered to be static during analysis after the hydroxymethylation and the formation of hemiformals virtually reached equilibrium. To control for a possible influence of condensation reactions, samples were prepared and analyzed at pH values of 7.5 and 8.5. Although literature reports the rate of condensation in UF mixtures to be negligible under neutral or basic conditions (Section on Main Reactions in the UF System), an increased fraction of condensation products was detected in samples prepared at a pH value of 7.5, compared with samples prepared at pH 8.5.

Synthesis of single components

Single components were prepared according to modified literature methods using non-enriched starting materials only. Thin-film chromatography was used to determine reaction progress during synthesis and to facilitate product purification. As none of the analytes show absorption in the UV-visible region, staining was required. The method described by Ludlam[50,91] gave very useful results (cf. Supporting Information). Table 1 lists the components that were synthesized and characterized. Details on synthesis and characterization are given in the Appendix.

Quantitative evaluation of the ^{15}N NMR spectra

All spectra were processed in the same way, with identical phase and baseline correction parameters. Based on the peak assign-

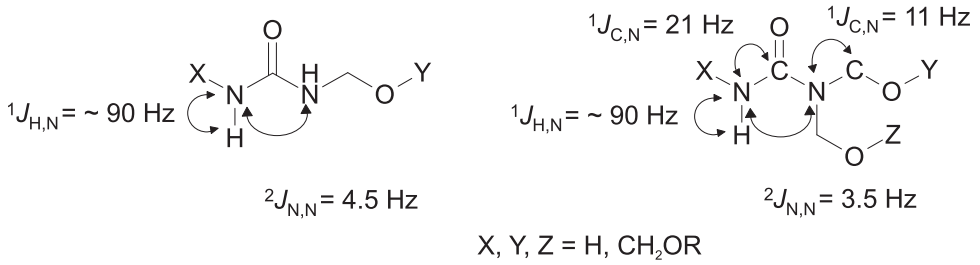

Figure 7. NMR spectroscopic coupling constants in monomethylol urea, as observed in this work.

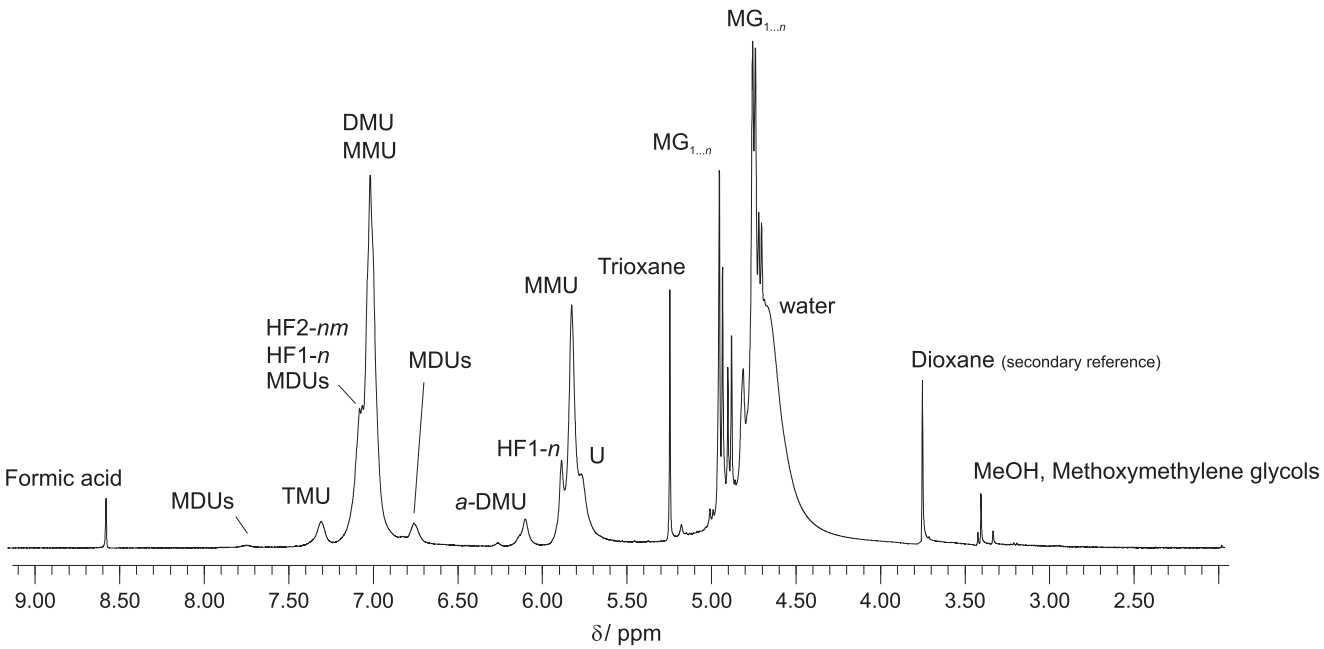

Figure 8. ^{1}H NMR spectrum of sample 2 (Table 2) and peak assignment (numerical data, cf. Tables 4–9); non-labeled urea was used here to avoid peak splitting due to large $^{1}J_{H,N}$.

ment described in the Peak Assignment, ^{1}H NMR Spectra, ^{13}N NMR Spectra, and ^{15}N NMR spectra sections, the spectra were integrated with standard integration routines provided by Varian's VNMR 6.1C spectrometer software, resulting in signal areas A_{ij} of the component *i* and its individual signals *j*. These signal areas can be directly used to calculate molar amounts because of the presence of the VR signal, which was referenced to a standard solution and represents a known molar amount of urea (Section 3.3). The individual areas A_{ij} of signal *j* and component *i* are divided by the stoichiometric correction factor z_i to yield molar amounts n_i:

$$n_i = \frac{A_{ij}}{z_i} \tag{1}$$

Here, the factor z_i is equal to the number of nitrogen centers in component *i*. The values for z_i are listed in Table 3. To describe the distribution of individual urea units NC(=O)N over the UF intermediates in the reaction mixture, pseudo-mole fractions $\hat{x}_{i,\mathrm{UF}}$ are introduced. From the available data, these are much easier to access than actual mole fractions x_i while being almost as useful to characterize the composition of the sample. The pseudo-mole fractions $\hat{x}_{i,\mathrm{UF}}$ are calculated as follows:

$$\hat{x}_{i,\mathrm{UF}} = \frac{n_i}{\sum_i n_{i,\mathrm{UF}} \cdot g_i} \tag{2}$$

It is assumed that $\sum_i n_{i,\mathrm{UF}} \cdot g_i$ is equivalent to the initial amount of urea $n_{0,\mathrm{U}}$. This assumption is valid if all UF intermediates are correctly identified and quantified. The factor g_i is the number of urea units NC(=O)N in component *i* and corrects for condensation products incorporating more than one urea unit. In this way, the distribution of the total initial amount of urea $n_{0,\mathrm{U}}$ among the reaction intermediates can be described. The values for g_i are listed in Table 3. The quantitative accuracy of these results is estimated to be 20% or better (relative deviation). The actual recovery rate (cf. Supporting Information) of urea was compared with the expected rate by using the VR signal. Smaller signals show a larger error and are easily overestimated because of integration errors correlated to low signal-to-noise ratio. In this work, the use of pseudo-mole fractions with reference to the concentrations of the starting materials and to the VR provided the only readily available path toward the composition of the mixtures. Despite its limitations regarding absolute accuracy, this approach proved to be a very valuable tool in describing the composition of the complex mixtures while keeping disturbance of the reaction equilibria at a minimum.

Quantitative evaluation of the ^{13}C NMR spectra

^{15}N NMR spectroscopy was combined with ^{13}C NMR spectroscopy to quantify nitrogen-free components. The target was to

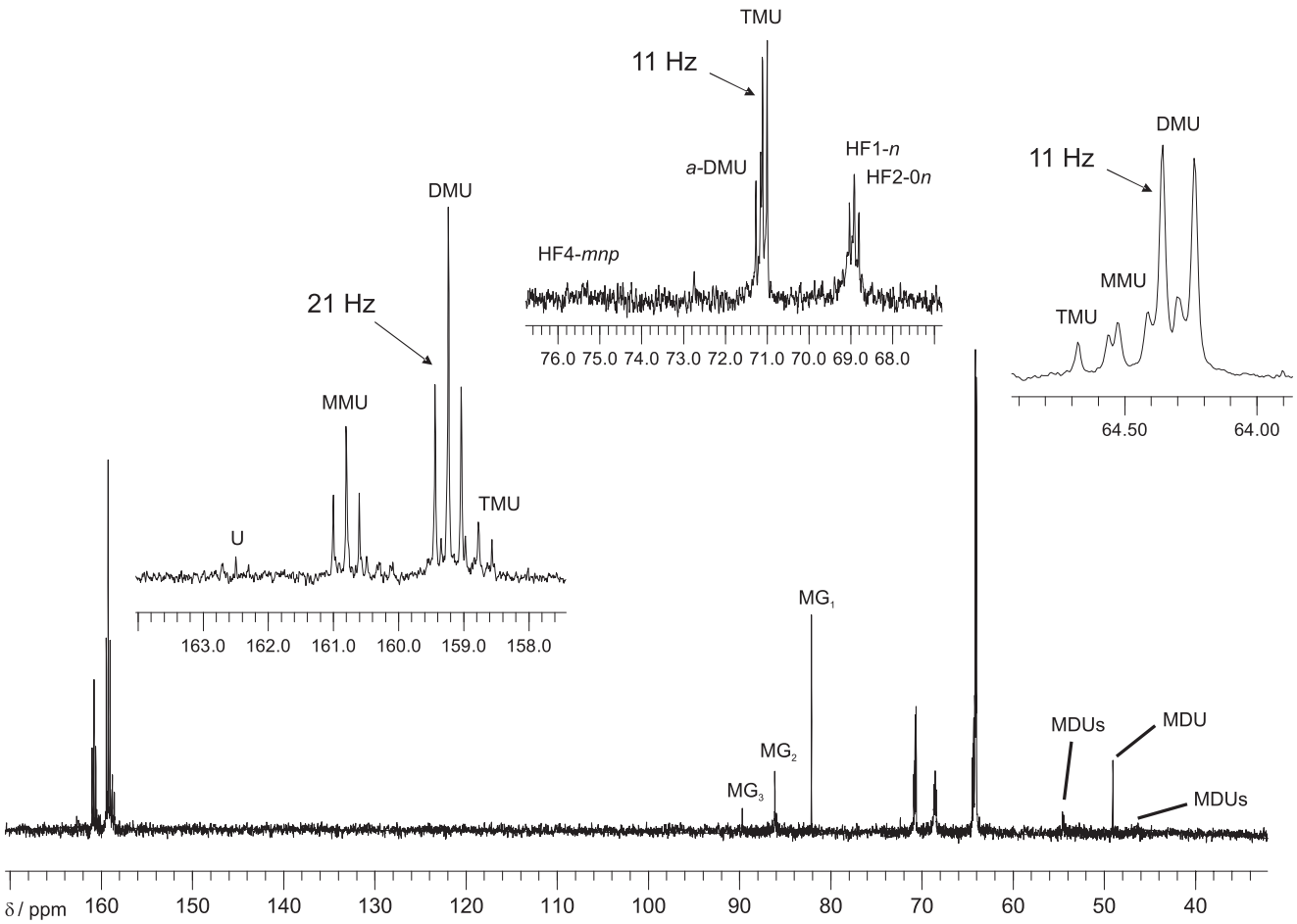

Figure 9. ^{15}N NMR spectrum of sample 3 (Table 2) and peak assignment (numerical data, cf. Tables 4–9); $^{2}J_{\mathrm{N,N}}$ splitting due to use of 98% ^{15}N-labeled urea.

complete the characterization of the samples by describing their composition in actual mole fractions x_i. A correlation was established between the ^{15}N and ^{13}C domains by means of signals of components occurring in both domains.

$$n_{i,\mathrm{FA}} = \frac{A_{ij}}{z_i} \cdot \frac{n_{MMU} + n_{DMU}}{A_{MMU} + A_{DMU}} \tag{3}$$

The factor z_i describes here the number of equivalent carbon centers giving rise to the signal A_{ij} (Table 3). These reference components were MMU and 1,3-bishydroxymethyl urea, which are both present in all samples in sufficiently large concentrations to enable reliable quantification. No VR signal was applied to the ^{13}C domain. The amounts of methylene glycols MG_1 to MG_3 were quantified in samples 1–7 (Table 2). After converting the resulting peak areas A_{ij} to molar amounts [cf. Eqn (1)], the pseudo-mole fractions $\hat{x}_{i,\mathrm{FA}}$ were calculated to describe the distribution of the initial amount of formaldehyde units CH_2O over the components in the reaction mixture in a way similar to what was performed for urea [cf. Eqn (2)]. As the initial FA/U ratio of the reaction mixture and the total amount of urea components in the mixture are known, the pseudo-mole fractions $\hat{x}_{i,\mathrm{FA}}$ are calculated based on the initial amount of formaldehyde in a similar manner as $\hat{x}_{i,\mathrm{UF}}$ (cf. Section on Quantitative Evaluation of the ^{15}N NMR Spectra):

$$\hat{x}_{i,\mathrm{FA}} = \frac{n_{i,\mathrm{FA}}}{n_{0,\mathrm{FA}}} \tag{4}$$

The initial amount of formaldehyde $n_{0,\mathrm{FA}}$ is here calculated using Eqn (5), provided all UF intermediates are correctly identified and quantified:

$$n_{0,\mathrm{FA}} = \frac{x_{0,\mathrm{FA}}}{x_{0,\mathrm{U}}} \cdot \sum_i n_{i,\mathrm{UF}} \cdot g_i \tag{5}$$

The pseudo-mole fractions of water present in the reaction mixture were calculated from Eqns (6–9):

$$\hat{x}_{i,\mathrm{W}} = \frac{n_{i,\mathrm{W}}}{n_{0,\mathrm{W}} + n_{\mathrm{W,cond.}} - n_{\mathrm{W,MGn}}} \tag{6}$$

$$n_{0,\mathrm{W}} = n_{0,\mathrm{U}} \cdot \frac{x_{0,\mathrm{W}}}{x_{0,\mathrm{U}}} \tag{7}$$

$$n_{\mathrm{W,cond.}} = \hat{x}_{\mathrm{MDUs}} \cdot n_{0,\mathrm{U}} \tag{8}$$

$$n_{\mathrm{W,MGn}} = \sum_i n_{i,\mathrm{MGn}} \tag{9}$$

The initial amount of water $n_{0,\mathrm{W}}$ originates from both the aqueous formaldehyde solution and the water content of the buffer solution. During the reaction, additional water $n_{\mathrm{W,cond.}}$ is formed via condensation of methylol components and urea to methylene diureas [MDUs, cf. Eqn (8)]. One mole of water is required to form one mole of methylene glycol. Hence, this amount of water has to be removed from the water balance [cf. Eqn (9)]. Table 2 lists the values for $x_{0,\mathrm{U}}$, $x_{0,\mathrm{FA}}$, and $x_{0,\mathrm{W}}$ for samples 1–7.

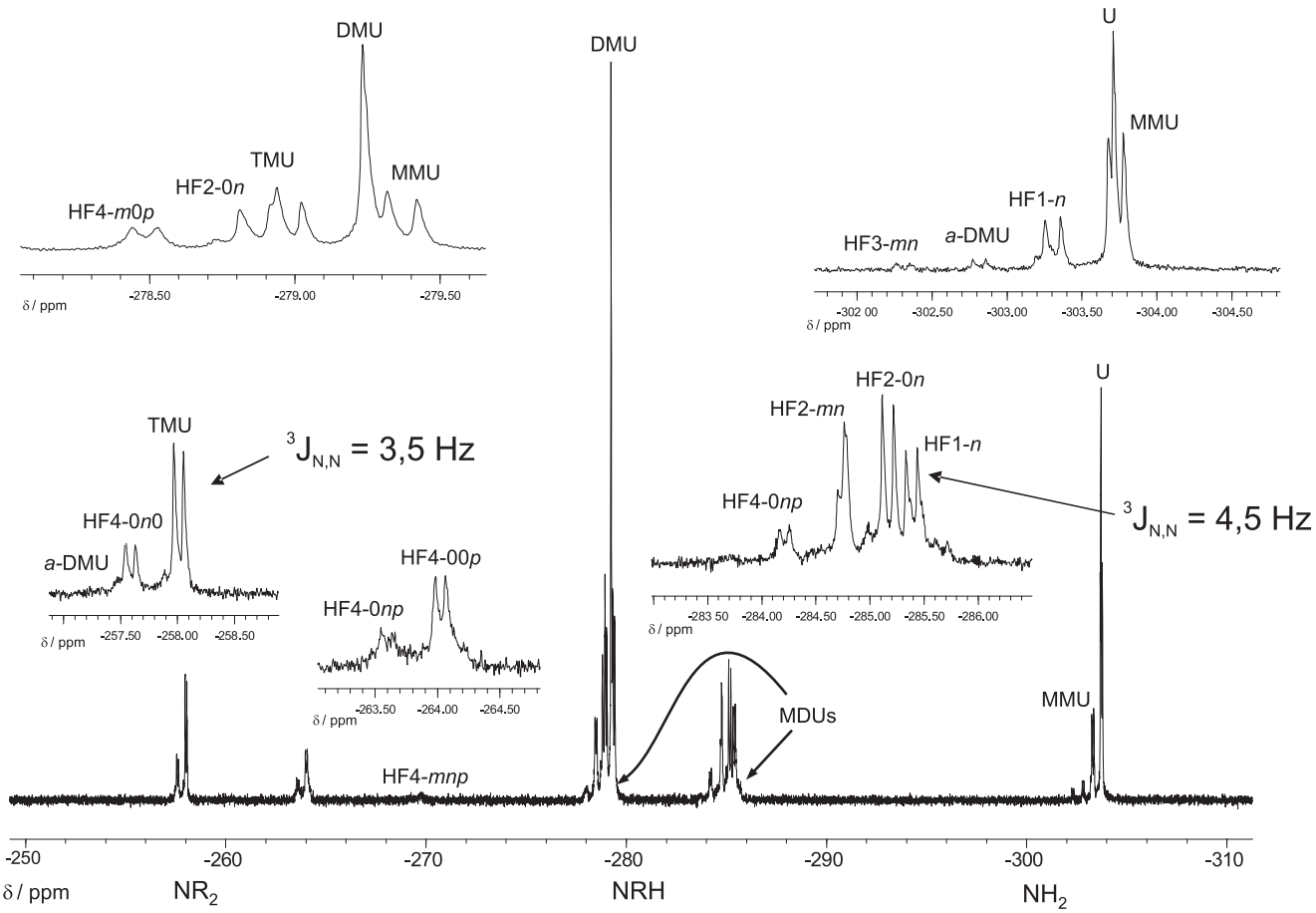

Figure 10. ^{15}N NMR spectrum of sample 3 (Table 2) and peak assignment (numerical data, cf. Tables 4–9); $^{2}J_{N,N}$ splitting due to use of 98% ^{15}N-labeled urea.

The actual mole fractions x_i were calculated as follows:

$$x_i = \frac{\hat{x}_{i,(\mathrm{UF,FA,W})}}{\sum_i \hat{x}_{i,\mathrm{UF}} + \sum_i \hat{x}_{i,\mathrm{FA}} + \frac{x_{0,\mathrm{W}}}{x_{0,\mathrm{U}}} \cdot \sum_i \hat{x}_{i,\mathrm{W}}} \quad (10)$$

The results are discussed in the Quantitative Analysis of 1D ^{15}N NMR Spectra and Quantitative Analysis of 1D ^{13}C NMR Spectra sections. The values $x_{0,\mathrm{U}}$, $x_{0,\mathrm{FA}}$, and $x_{0,\mathrm{W}}$ describe the overall fractions for urea, formaldehyde, and water, respectively. These are calculated from Eqns (11–13):

$$x_{0,\mathrm{U}} = \frac{n_{0,\mathrm{U}}}{n_{0,\mathrm{U}} + n_{0,\mathrm{FA}} + n_{0,\mathrm{W}}} \quad (11)$$

$$x_{0,\mathrm{FA}} = \frac{n_{0,\mathrm{FA}}}{n_{0,\mathrm{U}} + n_{0,\mathrm{FA}} + n_{0,\mathrm{W}}} \quad (12)$$

$$x_{0,\mathrm{W}} = 1 - x_{0,\mathrm{U}} - x_{0,\mathrm{FA}} \quad (13)$$

Results and Discussion

Peak assignment

First, the available single components (Table 1) were characterized by ^{1}H, ^{15}N, and ^{13}C NMR spectroscopy. With this information, the major peaks in the spectra of the reaction mixtures could be assigned (Table 2). Subsequently, the spectra for the samples with the three FA/U ratios 1, 2 and 4 were compared at pH 8.5. Sample 4, having the lowest formaldehyde content, contains the smallest number and the least complex of the UF intermediates. Here, complexity refers to the degree of substitution of urea and to the degree of addition of formaldehyde units to the hydroxymethyl substituents forming hemiformals. With increasing formaldehyde concentration, the number of different intermediates and their complexity increase. With this knowledge and with information on the $^2J_{\mathrm{N,N}}$ coupling constant and its dependence on the chemical environment, most of the peaks in the ^{15}N, ^{13}C, and ^{1}H spectra could be assigned. Comparing the spectra of mixtures of different pH values facilitated assignment of condensation products. 2D ^{15}N–^{15}N and 2D ^{13}C–{^{15}N} NMR spectroscopy were used to confirm the identity of peaks. Tables 4–9 provide a list of all identified components, together with their corresponding chemical shifts for all three studied nuclei as far as applicable and available.

Spin systems in UF intermediates

Figure 7 gives an overview on the two most relevant spin systems encountered in the reaction system. As the coupling constants are characteristic for the individual substitution patterns, their analysis proved to be valuable for peak assignment. It allows reliable assignment of signals of similar chemical shifts based on their spin

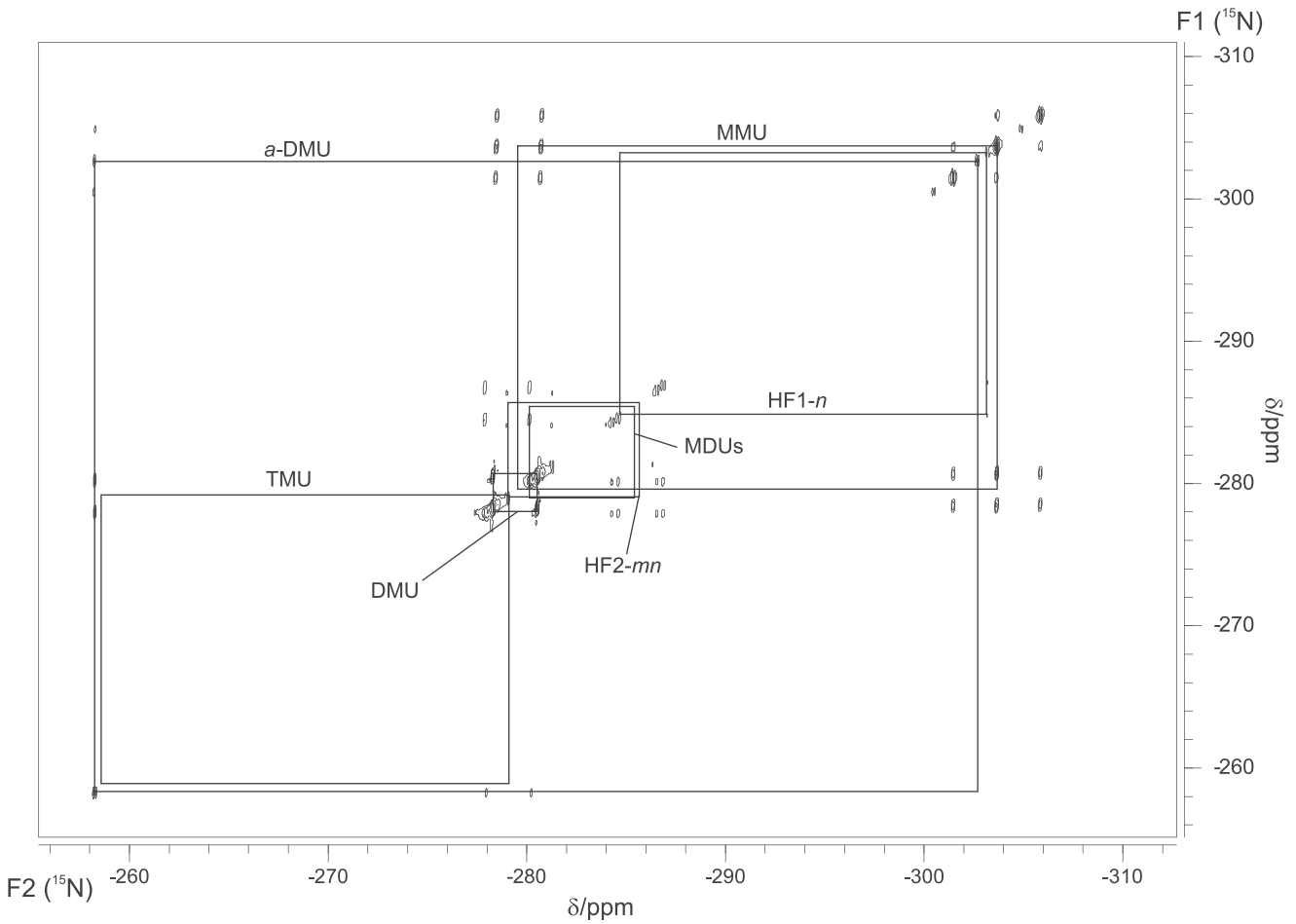

Figure 11. ^{15}N-TOCSY NMR spectrum of sample 3 (Table 2), no proton decoupling, 128 increments, four scans per increment, 0.06-s mixing time. The peak assignment via 1D NMR spectroscopy is confirmed.

environment. The first-order coupling constant $^{1}J_{H,N}$ was measured to be ~90 Hz. $^{1}J_{C,N}$ is ~21 Hz when a proton is present at nitrogen. It is ~11 Hz if this is not the case. The second-order coupling constant $^{2}J_{N,N}$ between the two nitrogen centers of the urea molecule was measured to be ~4.5 Hz if one or more protons are present at each of the nitrogen centers. It is ~3.5 Hz if one or both nitrogen centers are fully substituted.

^{1}H NMR spectra

Figure 8 shows the ^{1}H NMR spectrum of sample 2 (Table 2). The signals of the CH_2 groups originating from methylene glycols and urea-bound hydroxymethylene groups overlap strongly with each other and also with the broad water signal. The nitrogen-bound proton signals provide a much easier access to the mixture's composition, so only these were used for analysis. These signals exhibit much larger shifts with changes in their chemical environment when compared to the methylene protons. The observed signals of nitrogen-bound protons can be segregated into two groups, depending on the degree of substitution of the amide group. As urea has two amide groups, asymmetric intermediates exhibit a minimum of two resonances from nitrogen-bound protons. Single resonances originate from symmetric components or from derivatives with one fully substituted amino group. Condensates consisting of more than one urea unit can give rise to more than two signals, depending on their structure. As mentioned earlier, the first group of signals stems from unsubstituted amide groups and appears between 5.7 and 6.5 ppm. The signal of unsubstituted urea is found at 5.7 ppm. Substitution of one amide group of the urea molecule leads to a shift of the remaining unsubstituted group to a higher frequency. Hence, the signals of the unsubstituted amide groups of all derivatives will be shifted to a higher frequency compared to the urea signal. The second group of signals consists of the resonances originating from the partly substituted amide groups. These signals appear between 6.6 and 7.5 ppm.

^{13}C NMR spectra

Figure 9 shows the ^{13}C NMR spectrum of Sample 2. The signals form two major groups. The first group represents the carbonyl signals appearing between 158 and 163 ppm. The other represents the methylene groups and exhibits a rather wide range of shifts between 45 and 95 ppm, which is subdivided into three parts, each described in detail later. In the carbonyl signal group, the resonance of urea is found at the highest frequency of 162.5 ppm. Substitution of one proton on one amide group leads to a shift of 1.5 ppm toward lower frequencies. Each additional substitution causes a shift of 0.5 ppm toward lower frequencies, ultimately resulting in a resonance at 158.8 ppm for trihydroxymethyl urea. As the depicted spectrum was acquired from a sample containing ^{15}N-labeled urea, a first-order cou-

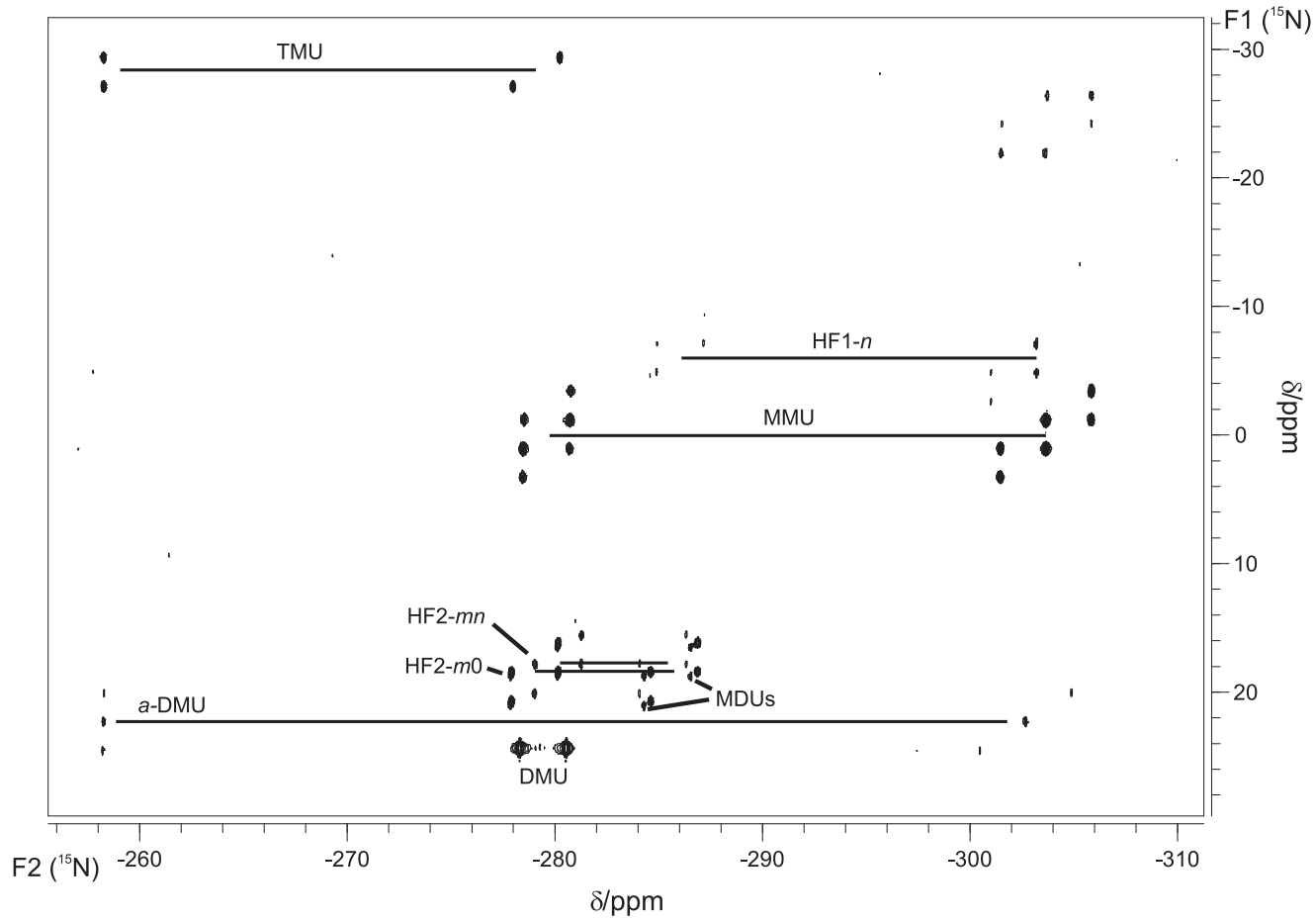

Figure 12. ^{15}N-INADEQUATE NMR spectrum of sample 3 (Table 2). No proton decoupling, 128 increments, 16 scans per increment. The peak assignment via 1D NMR spectroscopy is confirmed.

pling between ^{13}C and ^{15}N is present. Hence, all carbonyl signals appear as triplets with a coupling constant $^{1}J_{C,N}$ of 21 Hz (Fig. 7). The methylene range can be subdivided into three parts. From 45 to 60 ppm, the carbon centers of methylene bridges of the type N–CH_2–N appear. In the range of 64–76 ppm, resonances of hydroxymethyl groups of the types N–CH_2–OH and N–CH_2-O–R are found. Hydroxymethyl groups bound to a monosubstituted amide group appear between 64.3 and 64.6 ppm; the substitution pattern of the other amide groups leads to minor shifts here. Formation of a hemiformal by addition of formaldehyde to a hydroxymethyl group causes a shift to the higher frequency of 4 ppm, resulting in a signal group showing a resonance at ~69 ppm. Substitution of both protons of a NH_2 group with hydroxymethyl groups leads to a shift by ~7 ppm to a higher frequency over the monosubstituted amide, so the signals of the corresponding methylene groups appear between 71 and 72 ppm. In coherence with the previous finding, the resonance of the corresponding hemiformals is shifted by 4 ppm to the higher frequency of 75 ppm. Here, all methylene groups appear as doublets with a coupling constant of $^{1}J_{C,N} = 11$ Hz.

^{15}N NMR spectra

The ^{15}N NMR spectrum of sample 3 is illustrated in Fig. 10. In contrast to the previously described spectra, a sample with a high FA/U ratio was selected here to demonstrate the presence of a large number of signals originating from numerous hemiformals of hydroxymethyl intermediates. The observed resonances can be divided into three groups, each representing a specific degree of substitution. These groups are spaced at intervals of 24 ppm. They can be further divided into subgroups, corresponding to the nature of the substituent on the amide group. The signals of unsubstituted amide groups are found between −304 and −300 ppm (relative to CH_3NO_2), with unsubstituted urea resonating at the lowest frequency. Substitution on the other amide group of the molecule leads to shifts to a higher frequency by 0.4 ppm per additional hydroxymethyl group. Amide groups carrying a single hydroxymethyl group appear between −286 and −278 ppm in two subgroups: The signals of amide groups with hydroxymethyl substituents can be found between −280 and −278 ppm, while their corresponding hemiformals appear 6 ppm farther to the lower frequency. Fully substituted amide groups appear between −270 and −257 ppm in three subgroups spaced at 6 ppm. The amide groups bearing two hydroxymethyl groups contribute to the subgroup at the highest frequency at around −258 ppm. Amide groups with one hydroxymethyl group and one hemiformal form the subgroup at around −264 ppm, while the subgroup around −270 stems from amide groups with two hemiformal substituents. It should be noted that all resonances in the spectra taken from experiments employing ^{15}N-labeled urea are

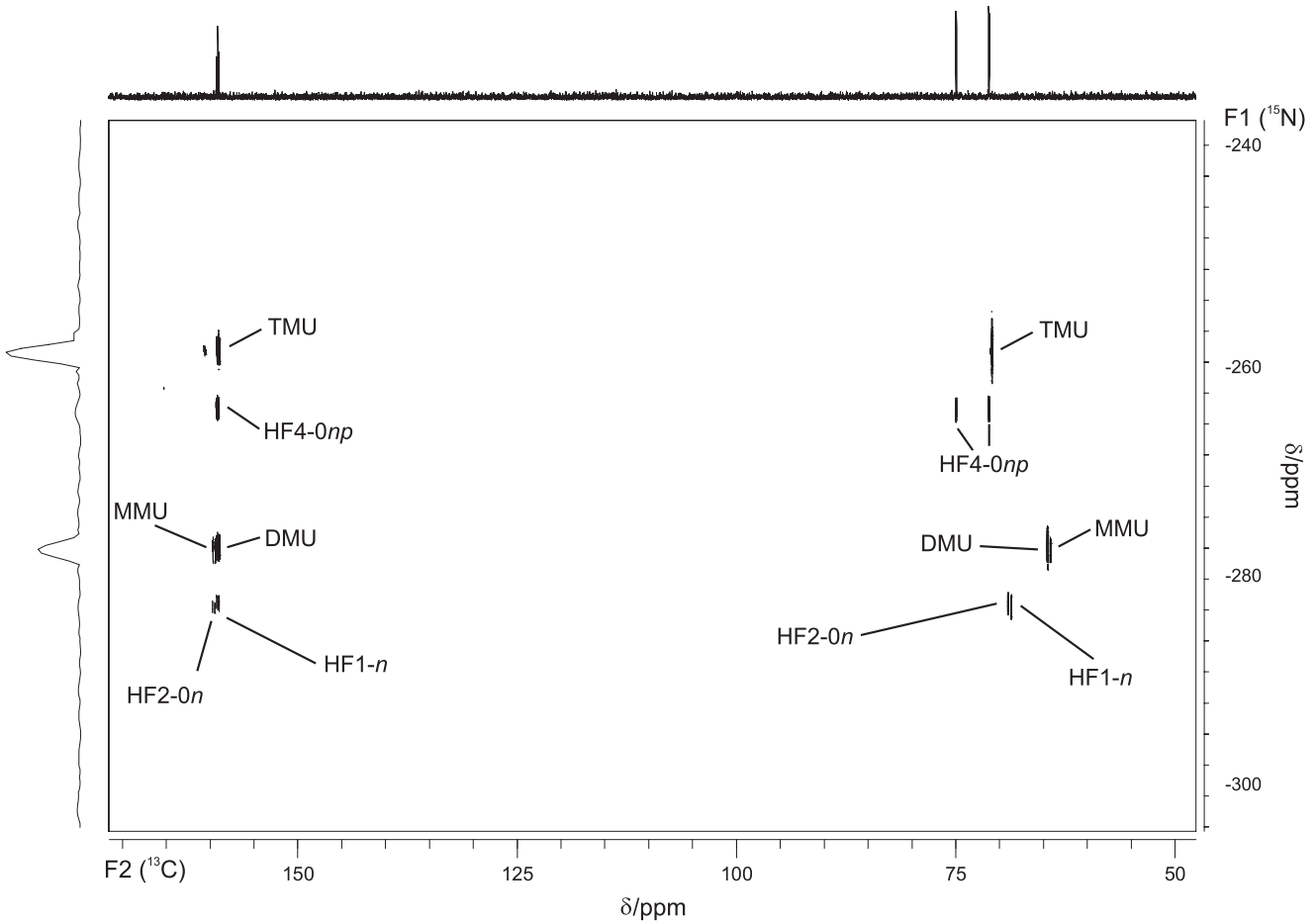

Figure 13. ^{13}C–{^{15}N}-gHMBC NMR spectrum of sample 3 (Table 2). ^{1}H-decoupled, 400 increments, 64 scans per increment. The peak assignment via 1D NMR spectroscopy is confirmed.

doublets with a coupling constant of either 3.5 or 4.5 Hz (symmetric components being the only exception). As described in the Section on Spin Systems in UF Intermediates, this is due to the $^{2}J_{N,N}$ coupling between the two ^{15}N centers. These couplings can be used to differentiate tertiary from secondary nitrogen centers. (In case a tertiary center is present, the coupling constant is 3.5 Hz. In all other cases, it is 4.5 Hz.) This additional information proved to be very useful assigning the 1D spectra and makes 2D NMR spectroscopy in the ^{15}N domain possible. Four examples of ^{15}N–^{15}N and ^{13}C–^{15}N correlation NMR spectroscopy are discussed here. Figure 11 shows a ^{15}N-TOCSY spectrum of sample 3. This spectrum confirms the peak assignment based on analysis of the coupling constants. Because of the FA/U ratio of 4, all methylol ureas, the hemiformals HF1 and HF2, and some MDUs can be identified. Figure 12 shows a ^{15}N-INADEQUATE NMR spectrum[92] of the same sample. The same components as in the ^{15}N-TOCSY NMR spectrum can be assigned. In both cases, no proton decoupling was used, as the patterns of the coupled signals facilitate peak assignment. Also, the $^{1}J_{C,N}$ and $^{1}J_{H,N}$ couplings can be utilized for correlation NMR spectroscopy. A ^{13}C–{^{15}N}-gHMBC NMR spectrum[93] of sample 3 is depicted in Fig. 13, linking the peak assignment between the ^{13}C and ^{15}N domains. Figure 14 depicts four ^{1}H–{^{15}N}-gHSQC NMR spectra of four reaction mixtures prepared from non-enriched urea at slightly different pH values than those in the samples listed in Table 2. Because of the indirect detection method and the high analyte concentrations, these spectra were acquired within 10–20 min. The difference between spectra A and B illustrates the influence of the pH value on the amount of MDUs. Spectra C and D demonstrate the influence of the FA/U ratio. In C, at an FA/U ratio of 4, only methylol ureas and their hemiformals are present; there is no unreacted urea. The spectrum of sample D in contrast contains significant amounts of unreacted urea and methylol ureas of low substitution degree. Also present are MDUs and small amounts of hemiformals. However, the main value of these ^{1}H–^{15}N correlations is the deconvolution of peaks in the ^{1}H domain with regard to individual components, as the degree of overlap is significant.

Determination of ^{15}N NMR chemical shift increments resulting from the addition of formaldehyde to NH_2 and NHR groups of urea and methylol ureas

Figure 15 illustrates the systematic changes in chemical shift in the ^{15}N NMR spectrum of NH_2 and NHR groups of urea and methylol ureas upon addition of formaldehyde to these components. Substitution of a proton on these functional groups with

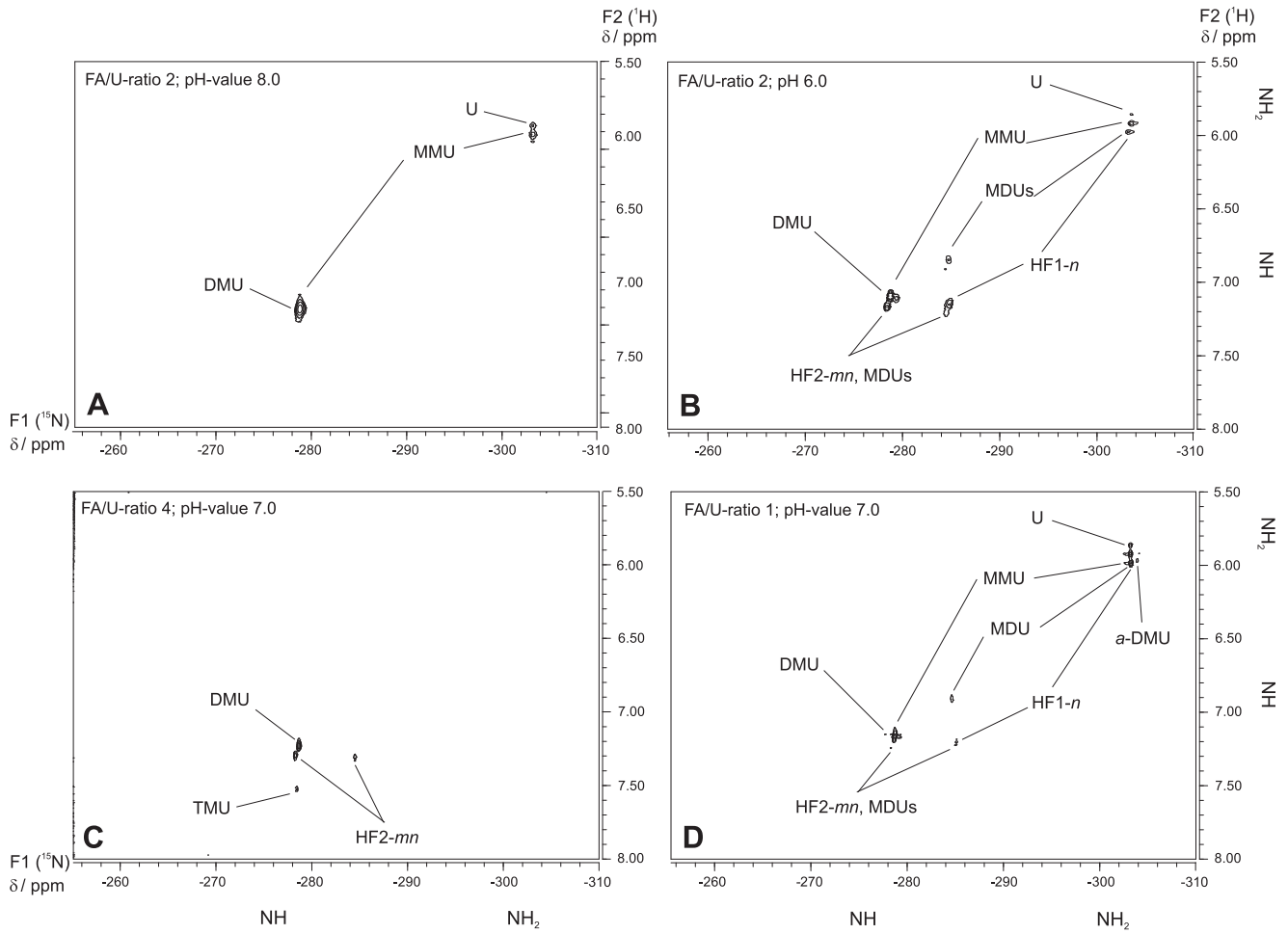

Figure 14. ^{1}H–{^{15}N}-gHSQC NMR spectra of four reaction mixtures prepared from non-enriched urea: (A) FA/U ratio 2, pH value 8.0; (B) FA/U ratio 2, pH value 6.0; (C) FA/U ratio 4, pH value 7.0; (D) FA/U ratio 1, pH value 7.0. Acquisition parameters: digital resolution of 1.4 pt/Hz in F2, 256 increments in F1, one scan per increment, 2-s repetition time, inverse gated decoupling on ^{15}N using the GARP sequence.

a hydroxymethyl group leads to a shift to the higher frequency of the directly affected nitrogen center of 24 ppm. The other (non-affected) nitrogen center is shifted to higher frequencies by 0.4–0.6 ppm, if it is not fully substituted itself. If it is a fully substituted tertiary nitrogen center (NR_2 group), it shifts by 0.4 ppm to lower frequencies. Addition of formaldehyde to hydroxymethyl groups leads to the corresponding hemiformals. This results in a shift to lower frequencies of 6 ppm, as compared to the directly affected nitrogen centers. The signals of the other, non-affected nitrogen centers shift by 0.4–0.6 ppm to higher frequencies if they are not fully substituted and 0.4 ppm to lower frequencies if they are fully substituted. The observed shifts in the ^{1}H and ^{13}C spectra are summarized in Table 10.

Quantitative analysis of 1D ^{15}N NMR spectra

Following the method described in the Quantitative Evaluation of the ^{15}N NMR Spectra section, pseudo-mole fractions $\hat{x}_{i,UF}$ were derived from the 1D ^{15}N NMR spectra. They represent the distribution of urea over the individual intermediates in the

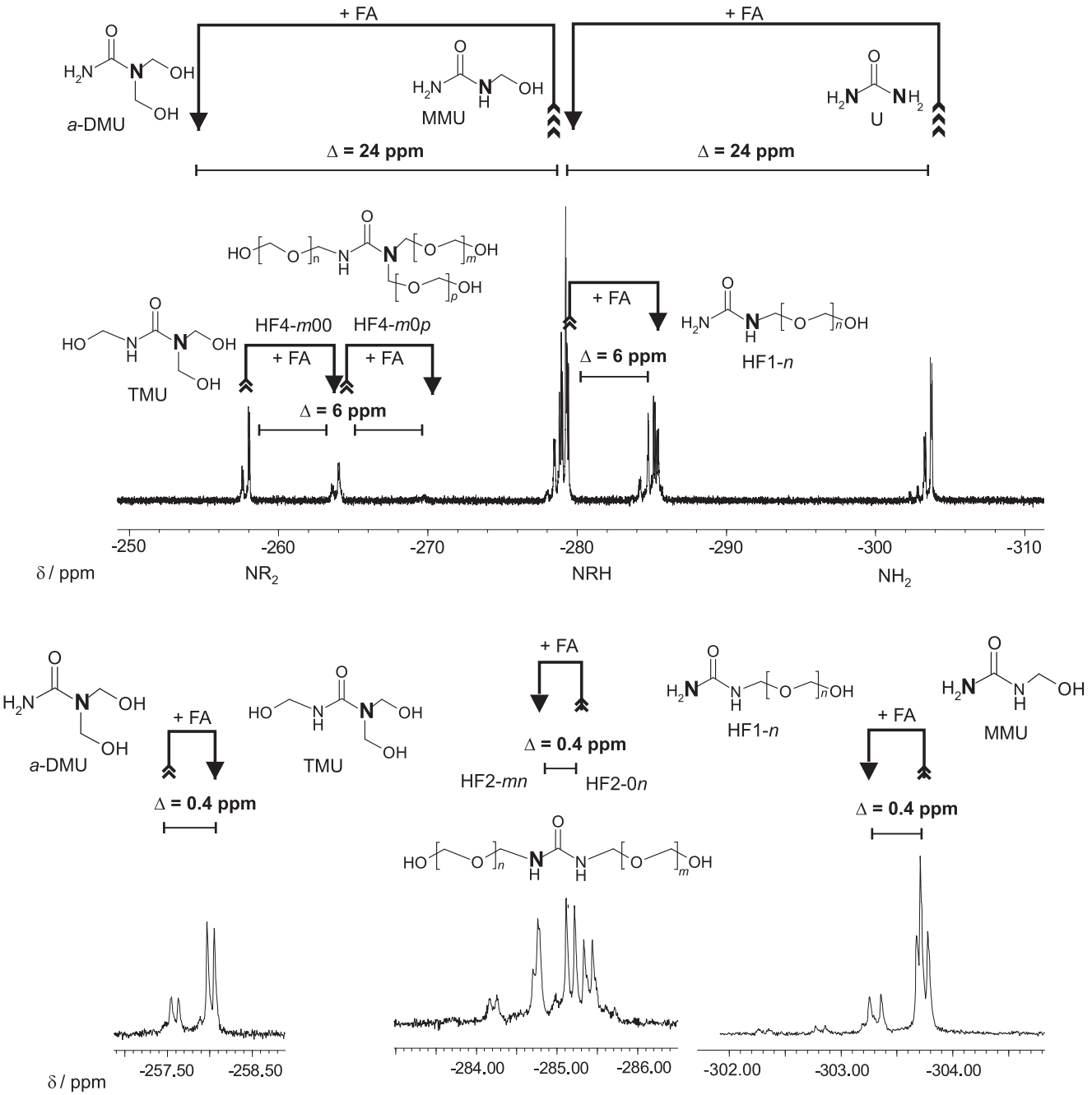

Figure 15. ^{15}N NMR chemical shift increments caused by addition of formaldehyde to urea and methylol ureas. The directly affected nitrogen centers shift by 24 ppm to higher frequencies, while the indirectly affected nitrogen centers shift only by 0.4 ppm. There is a shift of 6 ppm to the lower frequency upon addition of a formaldehyde unit to an existing hydroxymethyl group (cf. Table 10 for numerical data).

samples with regard to the initial amount of urea $n_{0,U}$ at the start of the reaction. Table 11 lists the numerical results. Figure 16 shows the ^{15}N NMR spectra of samples 1–3. Figure 17 depicts a graphical representation of the results for the distribution of urea in the samples. Figure 18 shows the corresponding ^{1}H NMR spectra.

- At FA/U ratio 1 and pH 7.5 (sample 1), 42% of the urea is present as MMU and 3.5% as its hemiformal (HF1-*n*). 15% exists as symmetric DMU and 5.5% as its hemiformal (HF2-0*n*). The asymmetric 1,1-DMU (*a*-DMU) contributes 1.5% to the total. About 3.6% is converted to MDU. However, 25% of the urea (U) is still present in its unreacted form in the mixture.
- At FA/U ratio 1 and pH 8.5 (sample 4), about 45% of the urea is converted to MMU and 2.2% to its hemiformal (HF1-*n*). 18% is present as symmetric DMU and 4.4% as its hemiformal (HF2-0*n*). Asymmetric 1,1-DMU (*a*-DMU) contributes at 1.4%. Only 1.3% is present as MDU.
- At FA/U ratio 2 and pH 7.5 (sample 2), the ratio between monosubstituted MMU and 1,3-DMU shifts in favor of the latter. MMU represents 22%, 1,3-DMU 34.4%, asymmetric 1,1-DMU (*a*-DMU) 3.4%, and TMU about 9% of the total, which amounts to about 70% of urea in the mixture. The hemiformal of MMU (HF1-*n*) represents 5.9%. The hemiformals of DMU, contributing 13.2%

Table 10. Changes in NMR chemical shifts upon addition of formaldehyde (Fig. 15)

	Nucleus/group					
	^{15}N (direct)	^{15}N (ind.)	^{13}C (CH_2)	^{13}C (C=O)	^{1}H (direct)	^{1}H (ind.)
Chemical shift	Δ / ppm					
$NH_2 \rightarrow NH(CH_2OH)$	24	0.6 (*tert.*: −0.4)	—	−1.5	1.3	0.06
$NH(CH_2OH) \rightarrow N(CH_2OH)_2$	24	0.6	7	−0.5	—	0.3
$NH(CH_2OH) \rightarrow$ HF1-*n*; HF2-0*n*	−6	0.4	4	<0.1	0.075	0.075
$N(CH_2OH)_2 \rightarrow$ HF3-0*n*; HF4-0*np*	−6	0.4	4	<0.1	—	n.a.
HF3-0*n* ; HF4-0*np* → HF3-*mn*; HF4-*mnp*	−6	0.4	4	<0.1	—	n.a.
HF1- *n* ; HF2-0*n* → HF3-0*n*; HF4-0*np*	24	0.6	6	−0.5	—	0.3

Table 11. Distribution of urea to different compounds described by pseudo-mole fractions $\hat{x}_{i,UF}$, $\hat{x}_{i,FA}$ and $\hat{x}_{i,W}$ based on the amount of urea at the start of the reaction $n_{0,Urea}$

Sample no.	1	2	3	4	5	6	7
FA/U ratio	1	2	4	1	1	2	4
Component	pH 7.5				pH 8.5		
	$\hat{x}_{i,UF}$ / mol · mol^{-1}						
U	0.253	0.027	—	0.270	0.268	0.036	—
MMU	0.420	0.224	0.052	0.450	0.447	0.277	0.060
DMU	0.150	0.344	0.314	0.177	0.173	0.435	0.296
a-DMU	0.015	0.034	0.027	0.014	0.020	0.041	0.027
TMU	—	0.092	0.247	—	—	0.086	0.231
HF1-*n*	0.035	0.059	—	0.022	0.024	0.045	0.006
HF2-0*n*	0.055	0.114	0.162	0.040	0.044	0.063	0.187
HF2-*mn*	—	0.018	0.048	—	—	0.011	0.045
HF4-*mn*0	—	0.018	0.091	—	—	—	0.102
HF4-0*np*	—	0.019	0.059	—	—	—	0.046
MDUs	0.036	0.026	—	0.013	0.012	0.003	—
	$\hat{x}_{i,FA}$ / mol · mol^{-1}						
MG_1	0.017	0.045	0.132	0.022	0.033	0.045	0.131
MG_2	—	0.010	0.041	—	—	0.013	0.041
MG_n	—	0.004	0.011	—	—	0.004	0.010
Total MG_n	0.017	0.059	0.184	0.022	0.033	0.062	0.182
	$\hat{x}_{i,W}$ / mol · mol^{-1}						
Water from condensation	0.002	0.002	—	0.001	0.001	—	—
Water bound in MG_n	−0.001	−0.005	−0.006	−0.002	−0.002	−0.006	−0.006
Initial water (FA solution + buffer)	0.999	1.003	1.006	1.001	1.001	1.005	1.006
Total water	1.0	1.0	1.0	1.0	1.0	1.0	1.0

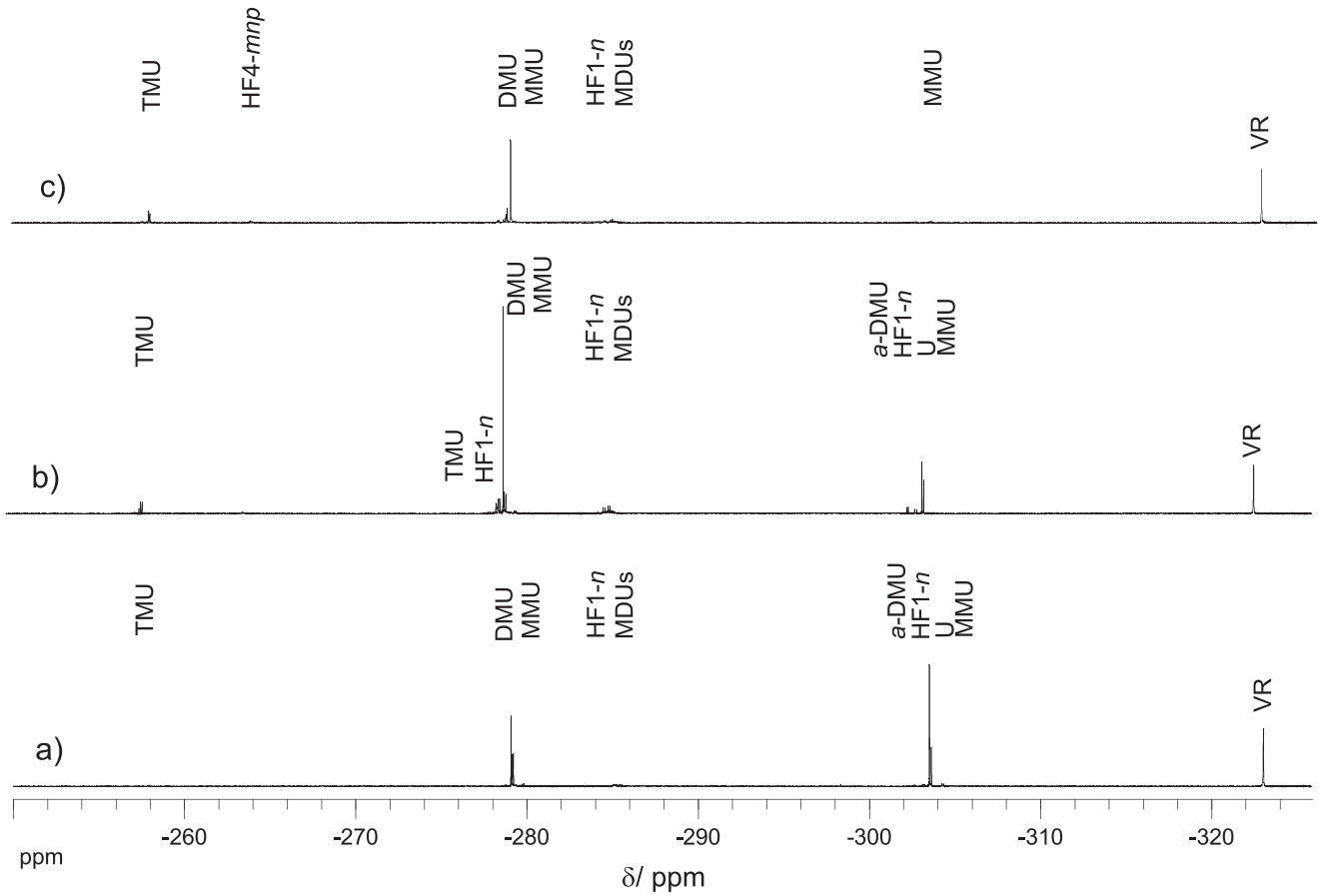

Figure 16. ^{15}N NMR spectra of (a) sample 1, (b) sample 2, and (c) sample 3 (FA/U ratios 1, 2, and 4; all pH 7.5, cf. Table 2).

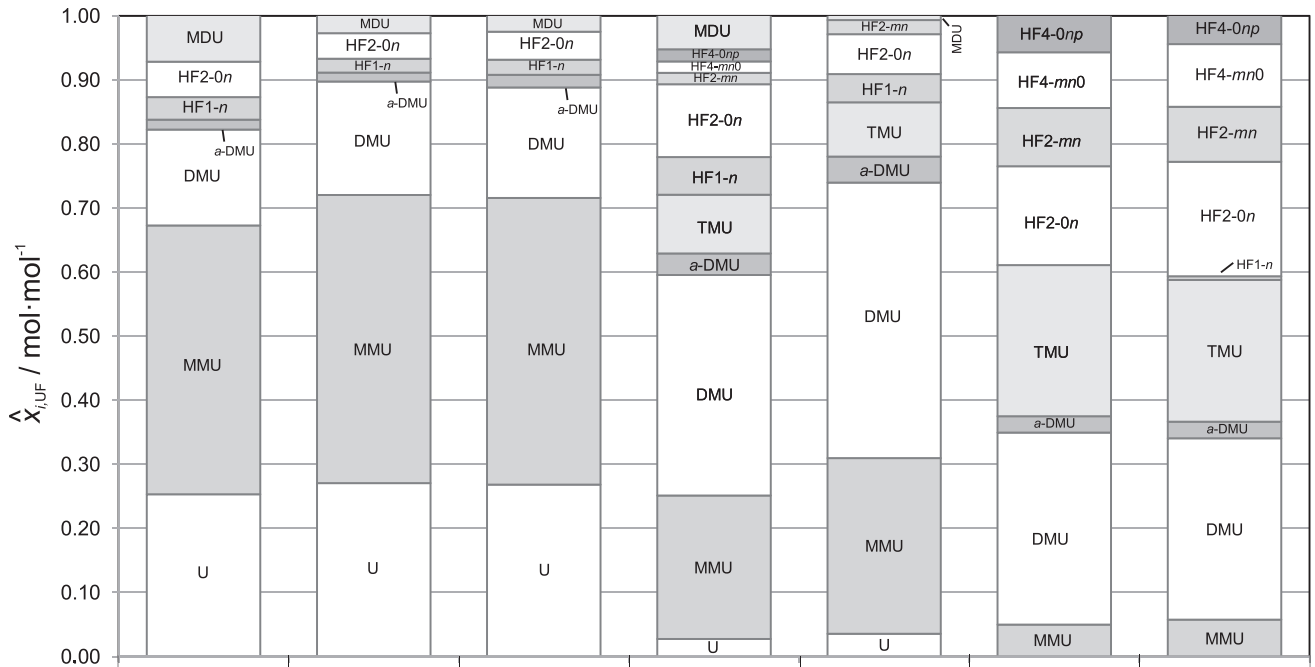

Figure 17. Distribution of urea to different compounds described by pseudo-mole fractions (cf. Tables 2 and 11).

together, can be subdivided into HF2-0*n*, which carries one oligomeric hydroxymethyl group, and HF2-*mn*, which carries two of these groups. These hemiformals contribute 11.4% and 1.8%. The hemiformals of TMU represent 3.7% of the total, consisting of 1.8% HF4-*mn*0 and 1.9% HF4-0*np*. Altogether, the hemiformals amount to 22.8% of the reaction mixture. Of total urea, 2.6% is present as MDU. Only 2.7% of urea (U) remains unreacted.

- At FA/U ratio 2 and pH 8.5 (sample 6), MMU represents 27.5%, 1,3-DMU 43%, asymmetric 1,1-DMU (*a*-DMU) 4.1%, and TMU about 8.5% of the total, which amounts to about 83.3% of urea in the mixture. The hemiformals here make up 12.8% of the total. The hemiformal of MMU (HF1-*n*) contributes 4.4%, and the hemiformals of DMU contribute 6.2% (HF2-0*n*) and 2.2% (HF2-*mn*). No HF4 was observed. Only 0.3% of urea is present as MDU, while 3.5% is present as unreacted urea (U).

- At FA/U ratio 4 and pH 7.5 (sample 3), no unreacted urea (U) was detected. 5% of total urea is present as MMU. The largest fraction exists as 1,3-DMU and TMU, contributing 30% and 23.6% to the total, respectively. Asymmetric 1,1-DMU (*a*-DMU) represents 2.6%. The hemiformals of DMU amount to 15.4% as HF2-0*n* and 9.1% as HF2-*mn*, while those of TMU contribute 8.7% as HF4-*mn*0 and 5.7% as HF4-0*np*. Together, the hemiformals amount to almost 38.9%. No hemiformal of MMU (HF1-*n*) and no MDUs were detected.

- At FA/U ratio 4 and pH 8.5 (sample 7), no unreacted urea (U) was detected. Of the total urea, 5.7% is present as MMU. 1,3-DMU represents 28.3%, asymmetric 1,1-DMU (*a*-DMU) 2.6%, and TMU 22.1% of the total urea. The hemiformals of DMU contribute 17.9% as HF2-0*n* and 8.6% as HF2-*mn* to the total, while those of TMU contribute to 9.8% as HF4-*mn*0 and 4.4% as HF4-0*np*. Together, the hemiformals amount to almost 41.3%. Only 0.3% hemiformal of MMU (HF1-*n*) and no MDU were detected. When comparing the composition of the samples taken at pH values 7.5 and 8.5, there is consistently more MDU present in the samples with pH 7.5, for a given FA/U ratio

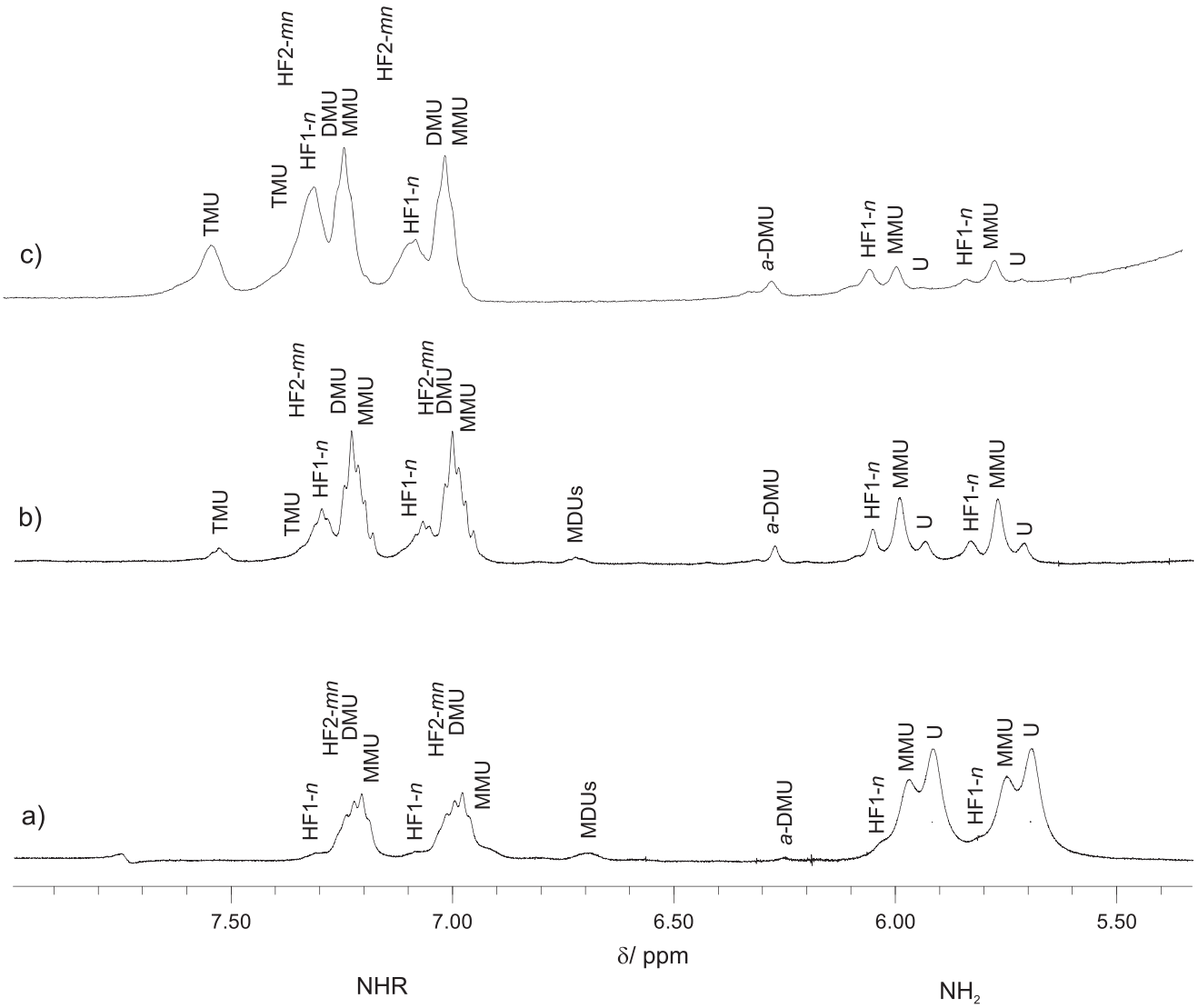

Figure 18. ^{1}H NMR spectra of (a) sample 1, (b) sample 2, and (c) sample 3 (FA/U ratios 1, 2, and 4; all pH 7.5, cf. Table 2) – only the spectral region of nitrogen-bound protons is shown.

(Section on Quantitative Analysis of 1D ^{13}C NMR Spectra and Table 12). This indicates a higher condensation rate at a lower pH value. Consequently, at this pH value, the fractions of MMU intermediates are decreasing, while the fractions of the corresponding hemiformals are increasing. The formation of one intermediate of the MDU type requires two urea units and one formaldehyde unit, which leads to the observed shift in composition. An increase in the FA/U ratio from 1 to 2 leads to a decrease in the fraction of unreacted urea (U) by one order of magnitude. The fraction of MMU also decreases by about 50%, while the fraction of DMU significantly increases. Also, the fractions of all hemiformals increase. TMU is detectable at an FA/U ratio of 2, while it is not present at an FA/U ratio of 1. There are differences in sample composition between pH 7.5 and 8.5, but comparing the different FA/U ratios at constant pH value reveals the same tendencies for both pH values.

At FA/U ratio 2, there is less MDU present. Despite an increase in formaldehyde content, the condensation rate is lower. Increasing the FA/U ratio from 2 to 4 leads to a concentration of urea (U) that is below the detection limit. Consequently, the fraction of hydroxymethylene urea (MMU) is also further reduced. The fraction of DMU decreased while the fraction of TMU increases significantly. The fractions of all hemiformals except HF1-*n* also increase. These observations are very similar for pH values 7.5 and 8.5. In both cases, no MDU is detected. The observed coexistence of DMU, hemiformals, and urea (U) is remarkable. The hydroxymethyl group shows a higher affinity toward formaldehyde than the amide group of unreacted urea. From the fact that a decrease in the fraction of unsubstituted NH_2 groups leads to a decrease in the fraction of condensation products, it may be concluded that the availability of both unsubstituted NH_2 groups and hydroxymethyl groups determines the rate of the condensation reaction.

Quantitative analysis of 1D ^{13}C NMR spectra

The 1D ^{13}C NMR spectra were analyzed in order to gain access to the concentration of unreacted formaldehyde in the samples, which is present in the form of methylene glycols (Fig. 19). Furthermore, with this information, the mole fractions x_i became accessible, which enable complete description of the sample's composition (Section on Quantitative Evaluation of the ^{13}C NMR spectra). The results are given in Table 12. The signals of the methylene glycols MG_1, MG_2, and MG_3 were evaluated, with MG_2, MG_3, and higher methylene glycols not being present at low FA/U ratios. This finding is in fair agreement with the results of Hahnenstein *et al.*[31] The primary parameter influencing the methylene glycol content of the mixtures is the FA/U ratio. At FA/U ratios of 1 and 2, only 2–3% and 4–5% of the initial amount of formaldehyde

Table 12. Composition of reaction mixtures given in mole fractions x_i

Sample no.	1	2	3	4	5	6	7
FA/U ratio	1	2	4	1	1	2	4
Component	pH 7.5				pH 8.5		
	x_i/ mol · mol^{-1}						
U	0.01597	0.00222	—	0.01705	0.01692	0.00291	—
MMU	0.02647	0.01827	0.00169	0.02837	0.02821	0.02259	0.00195
DMU	0.00943	0.02805	0.01024	0.01116	0.01088	0.03544	0.00964
a-DMU	0.00097	0.00274	0.00087	0.00089	0.00124	0.00335	0.00088
TMU	—	0.00747	0.00805	—	—	0.00698	0.00753
HF1-*n*	0.00221	0.00478	—	0.00136	0.00149	0.00365	0.00021
HF2-0*n*	0.00349	0.00928	0.00527	0.00252	0.00277	0.00513	0.00608
HF2-*mn*	—	0.00143	0.00156	—	—	0.00090	0.00146
HF4-*mn*0	—	0.00146	0.00297	—	—	—	0.00334
HF4-0*np*	—	0.00155	0.00194	—	—	—	0.00149
MDUs	0.00226	0.00212	—	0.00085	0.00077	0.00027	—
MG_1	0.00109	0.00366	0.00431	0.00141	0.00205	0.00366	0.00428
MG_2	—	0.00083	0.00133	—	—	0.00105	0.00135
MG_n	—	0.00029	0.00036	—	—	0.00033	0.00031
Water from condensation (equal to x_{MDUs})	0.00226	0.00212	—	0.00085	0.00077	0.00027	—
Water (other)	0.93812	0.91586	0.96141	0.93639	0.93568	0.91375	0.96147
Total	1.0	1.0	1.0	1.0	1.0	1.0	1.0
	Additional figures *(except for ratios subtotals of above balance, but not part of it)*						
Total UF intermediates (sum of above)	0.06079	0.07937	0.03259	0.06220	0.06227	0.08122	0.03259
Total unreacted FA as MG_n (sum of MG_n)	0.00109	0.00618	0.00805	0.00141	0.00205	0.00674	0.00791
Total FA bound to UF-intermediates	0.05970	0.15257	0.12229	0.06078	0.06022	0.15571	0.12243
Ratio FA bound/unbound	55	25	15	43	29	23	15
Total FA (unreacted + UF-bound)	0.06079	0.15874	0.13035	0.06220	0.06227	0.16244	0.13035
Subtotal FA bound in HFn	0.01487	0.05516	0.04165	0.01027	0.01128	0.02629	0.04383
Ratio FA HF/MG_n	13.7	8.9	5.2	7.3	5.5	3.9	5.5
Water bound in MG_n	−0.00109	−0.00477	−0.00600	−0.00141	−0.00205	−0.00503	−0.00594

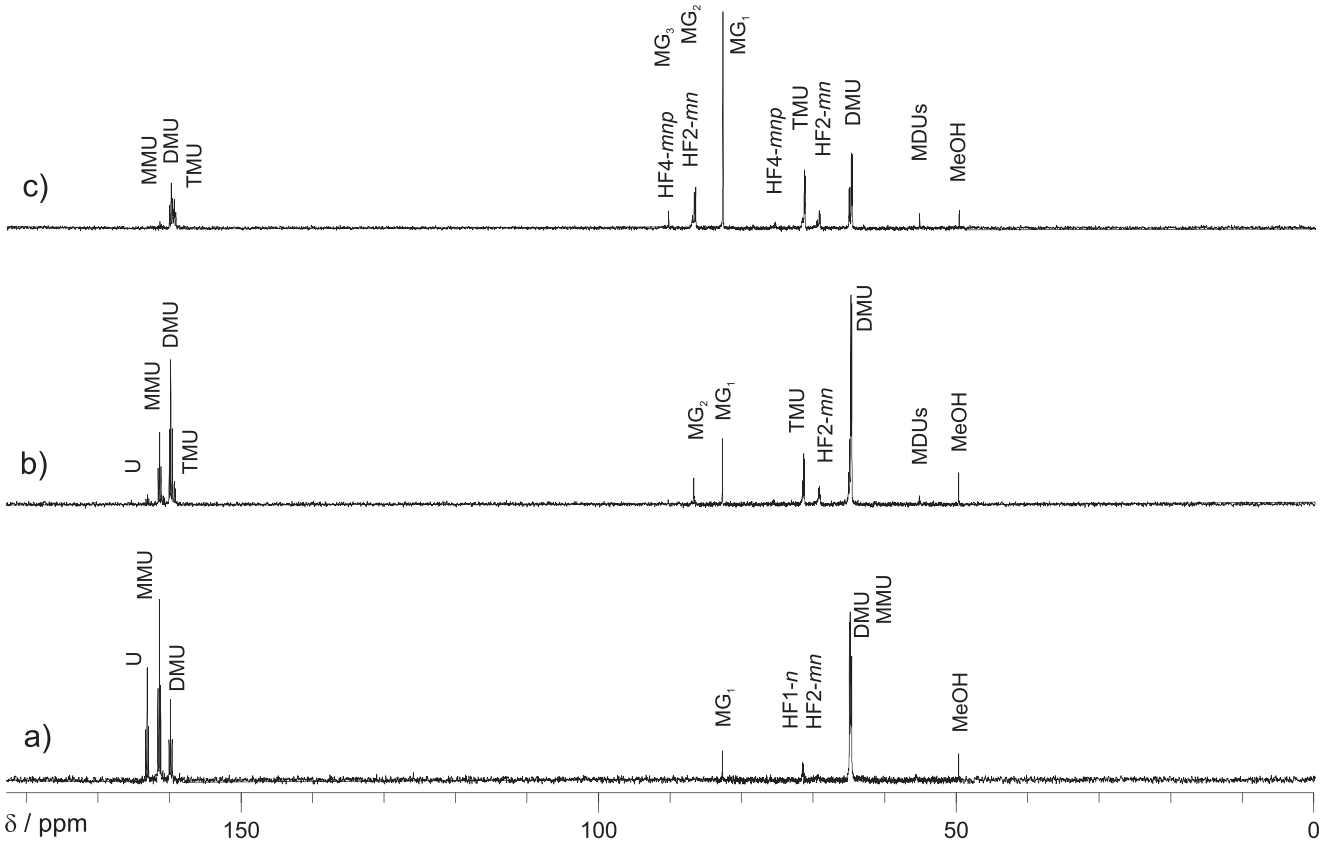

Figure 19. ^{13}C NMR spectra of (a) sample 1, (b) sample 2, and (c) sample 3 (FA/U ratios 1, 2, and 4; all pH 7.5, cf. Table 2).

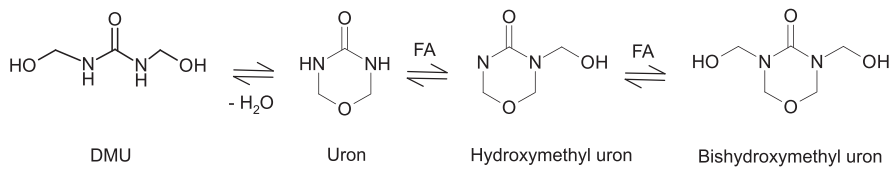

Figure 20. Formation of 1,3,5-oxadiazinanes (urons) and their hydroxymethyl derivatives.

do not react with urea. At an FA/U ratio of 4, this fraction increases to about 6–7%. It is remarkable that the ratio between formaldehyde bound in hemiformals of methylol ureas and formaldehyde bound in methylene glycols is rather high and varies between 3.9 and 13.7. Hence, the reaction of formaldehyde with hydroxymethyl groups is more favorable than the competing reaction with water, although the latter is present at a larger molar excess over methylol ureas.

Uron-type structures

Some authors postulate the formation of 1,3,5-oxadiazinan-4-on (uron) and its corresponding hydroxymethyl derivatives during various steps of the manufacturing process of UF resins.[39,75,78,94] Figure 20 shows the formation pathways of the three simplest examples of these intermediates. Formation of these components during the hydroxymethylation stage of the production process under the conditions described in the Sample and Preparation Analysis section could not be confirmed. However, it was possible to synthesize these structures via alternative methods and characterize them by NMR spectroscopy in the ^{1}H, ^{13}C, and ^{15}N domains. In the ^{13}C NMR spectrum, the resonances of these components are characteristic and straightforward to identify. Here, the carbonyl resonances are shifted toward lower frequencies when compared to non-cyclic intermediates and appear between 154.8 and 156.5 ppm. None of the reaction mixtures prepared in this study exhibited detectable levels of these components. Direct synthesis of dimethoxymethylene uron via intramolecular condensation of methylol ureas and subsequent removal of the methoxy hydroxymethyl groups succeeded (Section on Synthesis of Single Components and Appendix). However, considering the reaction conditions, it seems possible that these ring structures form during manufacture of fiber boards.

Conclusion

The hydroxymethylation stage of the synthesis of UF resins was studied by ^{1}H, ^{13}C, and ^{15}N NMR spectroscopy with regard to the distribution of intermediates and their identity. Several intermediates were identified for the first time by using 1D ^{15}N

NMR spectroscopy. The results were confirmed by 2D NMR spectroscopy and by direct synthesis. The change in ^{15}N chemical shift of the nitrogen centers of urea upon addition of formaldehyde was determined. The existence of hemiformals of methylol ureas was confirmed, and their chemical shifts were determined. No uron-type structures were identified under the studied conditions, but these structures were prepared otherwise and characterized. It was shown that reaction mixtures as they are commonly used in the industrial production of UF resins can be quantitatively analyzed by a combination of ^{15}N and ^{13}C NMR spectroscopy, resulting in a detailed description of the mixtures' composition at different feed ratios and pH values. The variation in pH value leads to a slight change in mixture composition due to the acid-catalyzed condensation reactions but did not measurably affect hydroxymethylation and formation of hemiformals. The results open a new route for characterizing the studied complex mixtures and ultimately for optimizing the UF resin production based on the knowledge of the true composition of the reacting mixtures.

References

[1] W. Keim, *Kunststoffe*, Wiley-VCH Verlag, Weinheim, Germany, **2006**.
[2] X. Tanga, Y. Bai, A. Duong, M. T. Smith, L. Li, L. Zhang, *Environ. Int.* **2009**, *35*, 1210–1224.
[3] M. Dunky, P. Niemz, *Holzwerkstoffe und Leime*, Springer-Verlag, Berlin Heidelberg, **2002**.
[4] H Kadowaki, *Bull. Chem. Soc. Jpn.* **1936**, *11*, 248–261.
[5] L. E. Smythe, *J. of Phys. and Colloid Chem.* **1947**, *51*, 369–378.
[6] L. E. Smythe, *J. Am. Chem. Soc.* **1951**, *73*, 2735–2738.
[7] L. E. Smythe, *J. Am. Chem. Soc.* **1953**, *75*, 1508–1510.
[8] G. A. Crowe, C. C. Lynch, *J. Am. Chem. Soc.* **1948**, *70*, 3795–3797.
[9] G. A. Crowe, C. C. Lynch, *J. Am. Chem. Soc.* **1949**, *71*, 3731–3733.
[10] J. de Jong, *Recl. Trav. Chim. Pay. B.* **1950**, *69*, 1566.
[11] J. de Jong, J. de Jonge, *Recl. Trav. Chim. Pay. B.* **1952**, *71*, 890–898.
[12] J de Jong, J de Jonge, *Recl. Trav. Chim. Pay. B.* **1952**, *71*, 643–660.
[13] J. de Jong, J. de Jonge, *Recl. Trav. Chim. Pay. B.* **1953**, *72*, 139–156.
[14] J. de Jong, J. de Jonge, *Recl. Trav. Chim. Pay. B.* **1953**, *72*, 169–172.
[15] J. de Jong, J. de Jonge, *Recl. Trav. Chim. Pay. B.* **1953**, *72*, 1027–1036.
[16] J. de Jong, J. de Jonge, *Recl. Trav. Chim. Pay. B.* **1953**, *72*, 213–217.
[17] J. de Jong, J. de Jonge, H. A. K. Eden, *Recl. Trav. Chim. Pay. B.* **1952**, *71*, 661–667.
[18] J. de Jong, J. de Jonge, H. A. K. Eden, *Recl. Trav. Chim. Pay. B.* **1953**, *72*, 88–90.
[19] N. Landqvist, *Acta Chem. Scand.* **1955**, *9*, 1127–1142.
[20] N. Landqvist, *Acta Chem. Scand.* **1955**, *9*, 1459–1465.
[21] N. Landqvist, *Acta Chem. Scand.* **1955**, *9*, 1466–1470.
[22] N. Landqvist, *Acta Chem. Scand.* **1955**, *9*, 1471–1476.
[23] N. Landqvist, *Acta Chem. Scand.* **1955**, *9*, 1477–1483.
[24] N. Landqvist, *Acta Chem. Scand.* **1956**, *10*, 244–248.
[25] N. Landqvist, *Acta Chem. Scand.* **1957**, *11*, 776–779.
[26] N. Landqvist, *Acta Chem. Scand.* **1957**, *11*, 792–803.
[27] N. Landqvist, *Acta Chem. Scand.* **1957**, *11*, 780–785.
[28] N. Landqvist, *Acta Chem. Scand.* **1957**, *11*, 786–791.
[29] R. Kveton, *Collect. Czech. Chem. Commun.* **1956**, *21*, 593–606.
[30] BFA, Formaldehyd – Gefährlicher als bisher angenommen? Stellungnahme vom 29. November 2004, **2004**.
[31] I. Hahnenstein, M. Albert, H. Hasse, C. G. Kreiter, G. Maurer, *Ind. Eng. Chem. Res.* **1995**, *34*, 440–450.
[32] H. Hasse, G. Maurer, *Ind. Eng. Chem. Res.* **1991**, *30*, 2195–2200.
[33] J. F. Walker, *Formaldehyde* (3ed.), ACS Monograph Series, Reinhold Publishing Corporation, New York City, **1964**.
[34] M. Chiavarini, N. Delfanti, R. Bigatto, *Angew. Makromol. Chem.* **1975**, *46*, 151–162.
[35] S. M. Kambanis, R. C. Vasishth, *J. Appl. Polym. Sci.* **1971**, *15*, 1911–1919.
[36] W. Dankelman, J. M. H. Daemen, A. J. J. de Breet, J. L. Mulder, W. G. B. Huysmans, J. de Wit, *Angew. Makromol. Chem.* **1976**, *54*, 187–201.
[37] A. J. J. de Breet, W. Dankelman, W. G. B. Huysmans, J. de Wit, *Angew. Makromol. Chem.* **1977**, *62*, 7–31.
[38] J. R. Ebdon, P. E. Heaton, *Polymer* **1977**, *18*, 971–974.
[39] B. Tomita, S. Hatono, *J. Polym. Sci., Part A: Polym. Chem.* **1978**, *16*, 2509–2525.
[40] R. Rammon, W. E. Johns, J. Magnuson, K. Dunker, *J. Adhesion* **1986**, *19*, 115–135.
[41] M. G. Kim, L. W. Amos, *Chem. Ber.* **1990**, *29*, 208–212.
[42] P. Christjanson, T. Pehk, K. Siimer, *J. Appl. Polym. Sci.* **2006**, *100*, 1673–1680.
[43] K. Siimer, P. Christjanson, T. Kaljuvee, T. Pehk, I. Lasn, I. Saks, *J. Therm. Anal. Calorim.* **2008**, *92*, 19–27.
[44] A. Despres, A. Pizzi, H. Pasch, A. Kandelbauer, *J. Appl. Polym. Sci.* **2007**, *106*, 1106–1128.
[45] J. Ebdon, P. E. Heaton, T. N. Huckerby, W. T. S. O'Rourke, J. Parkin, *Polymer* **1984**, *25*, 821.
[46] J. Ebdon, B. J. Hunt, W. T. S. O'Rourke, J. Parkin, *Brit. Polym. J.* **1988**, *20*, 327–334.
[47] R. A. Thomson, M. Manley-Harris, B. D. Gill, *Magn. Reson. Chem.* **2003**, *41*, 622–625.
[48] A. S. Angelatos, M. I. Burgar, N. Dunlop, F. Separovic, *J. Appl. Polym. Sci.* **2004**, *91*, 3504–3512.
[49] A. Philbrook, C. J. Blake, N. Dunlop, C. J. Easton, M. A. Keniry, J. S. Simpson, *Polymer* **2005**, *46*, 2153–2156.
[50] O. Steinhof, *NMR-spektroskopische Aufklärung des bei der Umsetzung von Harnstoff mit Formaldehyd auftretenden Reaktionsnetzwerks*. PhD Thesis, Cuvillier Verlag Göttingen, Universität Stuttgart, **2010**.
[51] E. J. Kibrik, O. Steinhof, G. Scherr, W. R. Thiel, H. Hasse, *Ind. Eng. Chem. Res.* **(submitted 2014)**.
[52] H. G. Schecker, W. Jost, *Ber. Bunsen-Ges. Phys. Chem.* **1969**, *73*, 521–526.
[53] H. G. Schecker, G. Schulz, *Z. Phys. Chem. (Frankfurt, Ger.)* **1969**, *65*, 221–224.
[54] I. Hahnenstein, H. Hasse, C. G. Kreiter, G. Maurer, *Ind. Eng. Chem. Res.* **1994**, *33*, 1022–1029.
[55] I. Hahnenstein, H. Hasse, Y.-Q. Liu, G. Maurer, *AIChE Symp. Ser.* **1994**, *90*, 141–157.
[56] H. Dahn, P. Pechy, *Magn. Reson. Chem.* **1996**, *34*, 723–724.
[57] M. Maiwald, H. H. Fischer, Y. K. Kim, H. Hasse, *Anal. Bioanal. Chem.* **2003**, *375*, 1111–1115.
[58] M. Maiwald, H. H. Fischer, M. Ott, R. Peschla, C. Kuhnert, C. G. Kreiter, G. Maurer, H. Hasse, *Ind. Eng. Chem. Res.* **2003**, *42*, 259–266.
[59] C. Kuhnert, M. Albert, S. Breyer, I. Hahnenstein, H. Hasse, G. Maurer, *Ind. Eng. Chem. Res.* **2006**, *45*, 5155–5164.
[60] S. Cannizzaro, *Liebigs Ann. Chem.* **1853**, *88*, 129–130.
[61] D. Luther, H. Koch, *Chem. Ber.* **1966**, *99*, 2227–2236.
[62] M. Ott, H. H. Fischer, M. Maiwald, K. Albert, H. Hasse, *Chem. Eng. Process.* **2005**, *44*, 653–660.
[63] B. R. Glutz, H. Zollinger, *Helv. Chim. Acta* **1969**, *52*, 1976–1984.
[64] E. J. Kibrik, O. Steinhof, G. Scherr, W. R. Thiel, H. Hasse, *J. Appl. Polym. Sci.* **2012**, *128*, 3957–3963.
[65] E. J. Kibrik, O. Steinhof, G. Scherr, W. R. Thiel, H. Hasse, *J. Polym. Res.* **2013**, *20*, 1–10.
[66] P. Christjanson, I. Lasn, K. Siimer, T. Pehk, *Holz als Roh- und Werkstoff* **2002**, *60*, 379–384.
[67] P. Christjanson, T. Pehk, K. Siimer, *Proc. Estonian Acad. Sci. Chem.* **2006**, *55*, 212–225.
[68] I. S. Chuang, G. E. Maciel, *Macromolecules* **1992**, *25*, 3204–3226.
[69] C. Goldschmidt, *J. Prakt. Chem.* **1897**, *46*, 460.
[70] K. Siimer, T. Pehk, P. Christjanson, *Macromol. Symp.* **1999**, *148*, 149–156.
[71] G. Zigeuner, H. Fitz, *Monatsh. Chem.* **1959**, *90*, 211–221.
[72] V. Horn, G. Benndorf, K. P. Rädler, *Plaste Kautsch* **1978**, *25*, 570–575.
[73] R. Kveton, *Collect. Czech. Chem. Commun.* **1959**, *24*, 2068–2071.
[74] T. Mejdell, H. K. Schjønsby, *Macromol. Symp.* **2004**, *206*, 241–254.
[75] C. Soulard, C. Kamoun, A. Pizzi, *J. Appl. Polym. Sci.* **1999**, *72*, 277–289.
[76] G. Zigeuner, W. Knierzinger, K. Voglar, E. Wiesenberger, M. Sobotka, *Monatsh. Chem.* **1951**, *82*, 847–855.
[77] M. T. Beachem, P. D. Schickedanz, J. C. Oppelt, D. V. Maier, F. M. Cowen, *J. Org. Chem.* **1963**, *28*, 1876.
[78] W. Gao, J. Li, *Maderas. Ciencia y Tecnologia* **2012**, *14*, 3–12.
[79] J. H. Meessen, *Ullmann's Encyc. of Indust. Chem.* **2010**, *37*, 657–693. DOI: 10.1002/14356007.a27_333.pub2
[80] R. K. Harris, E. D. Becker, S. M. C. D. Menezes, R. Goodfellow, P. Granger, *Pure Appl. Chem.* **2001**, *73*, 1795–1818.
[81] T. D. Claridge, *High-resolution NMR Techniques in Organic Chemistry* (1st edn), Elsevier Ltd., Oxford, **1999**.

[82] F. Malz, *Quantitative NMR-Spektroskopie als Referenzverfahren in der analytischen Chemie*. PhD Thesis, Humboldt-Universität zu Berlin, **2003**.
[83] F. Malz, H. Jancke, *J. Pharm. Biomed. Anal.* **2005**, *38*, 813–823.
[84] M. Maiwald, *Hochauflösende Online-NMR-Spektroskopie für das Reaktions- und Prozeßmonitoring - Beispiele zur Anwendung in der Verfahrenstechnik*, Habilitation. Cuvillier Verlag Göttingen, Technische Universität Kaiserslautern, **2012**.
[85] M. Maiwald, O. Steinhof, H. Hasse, *Nachr. Chem.* **2007**, *55*, 745–749.
[86] M. Maiwald, O. Steinhof, C. Sleigh, M. Bernstein, H. Hasse, *Quantitative High-resolution Online NMR Spectroscopy in Pharmaceutical Reaction and Process Monitoring* (Eds: U. Holzgrabe, I. Wawer, B. Diehl), Chapter 8, vol. NMR Spectroscopy in Pharmaceutical Analysis, Elsevier, **2008**, pp. 471–491.
[87] R. K. Harris, E. D. Becker, S. M. C. D. Menezes, P. Granger, R. E. Hoffman, K. W. Zilm, *Pure Appl. Chem.* **2008**, *80*, 59–84.
[88] H. P. Mahon, *Rev. Sci. Instrum.* **1969**, *40*, 1644–1645.
[89] S. Akoka, L. Barantin, M. Trierweiler, *Anal. Chem.* **1999**, *71*, 2554–2557.
[90] I. Billault, R. Robins, S. Akoka, *Anal. Chem.* **2002**, *74*, 5902–5906.
[91] P. R. Ludlam, *Analyst* **1973**, *98*, 107–115.
[92] J. Buddrus, H. Bauer, *Angew. Chem., Int. Ed.* **1987**, *26*, 625–642.
[93] W. P. Niemczura, G. L. Helms, A. S. Chesnick, R. E. Moore, V. Bornemann, *J. Magn. Reson.* **1989**, *81*, 635–640.
[94] B. Tomita, Y. Hirose, *J. Polym. Sci., Part A: Polym. Chem.* **1976**, *14*, 387–401.
[95] T. P. Murray, *J. Labelled Compd. Radiopharm.* **1985**, *22*, 1251–1259.
[96] A. M. Paquin, *J. Org. Chem.* **1949**, *14*, 189–193.

Appendix

Synthesis of single components

Monomethylol urea

Synthesis, workup, and purification are carried out following the procedure of de Jong and de Jonge[12]; a yield of 26.6% with regard to urea was obtained. An amount of 540 g of urea was dissolved in 375 g of distilled water and cooled to 5 ° C. The pH value was adjusted to 8.0 using an automated pH control system dosing aqueous solutions of sodium hydroxide and formic acid to keep the pH value constant. Over the course of 1 h, 676 g of an aqueous solution of formaldehyde ($x_{0,FA}$ = 0.3 g/g) was added while keeping the temperature below 25 °C. Workup and purification was performed as described by de Jong and de Jonge. This resulted in 221 g of MMU of a purity exceeding 90%, which corresponds to a yield of 26.6% with regard to urea.

TLC: R_f = 0.30 (green spot); ^{1}H NMR (H_2O): δ = 7.1 (bt, J = 7.0 Hz, 1H, $OCH_2N\underline{H}$); 5.9 (2H, $N\underline{H}_2$); 4.64 (d, J = 7.0 Hz, 2H, $OC\underline{H}_2NH$). ^{13}C NMR (H_2O): δ = 160.8 (1C, $\underline{C}$=O); 64.3 (1C, $\underline{C}H_2$). ^{15}N NMR (H_2O): $\delta_{CD_3NO_2}$ = −280.7 (d, $^{1}J_{N,H}$ = |91, 5| Hz, $OCH_2\underline{N}H$,); -304.8 (t, $^{1}J_{N,H}$ = |89.2| Hz, $\underline{N}H_2$). Melting point: 110 °C.

1,3-Bishydroxymethyl urea (DMU)

An amount of 400 g of an aqueous formaldehyde solution ($x_{0,FA}$ = 0.3g/g) was adjusted to 5 °C and a pH value of 8.0. Then, 120 g of solid urea was added sufficiently slowly to keep the temperature below 25 °C. The pH value was kept at 8.0 by means of the automatic pH control system mentioned earlier. After 2 h of stirring, the mixture was stored at 0 °C for 16 h. Then, water was evaporated under vacuum until the volume was reduced to 50% while keeping the temperature below 50 °C. The precipitate was removed and washed once with ethanol and then once with diethyl ether. A second fraction of solid was obtained by storing the mother liquors at 0 °C for 24 h. This was washed in the same way. Both fractions were combined and recrystallized from 1.5 l of a mixture of ethanol and diethyl ether at a ratio of 3 : 2 with 1 g of K_3PO_4 added as a buffer. In total, 107.8 g of the target component with 95% purity was obtained. This represents a yield of 43% with regard to urea.

TLC: R_f= 0.21 (yellow spot); ^{1}H NMR (D_2O): δ = 7.1 (bt, J = 6.8 Hz, 2H, $OCH_2N\underline{H}$); 4.69 (d, J = 6.8 Hz, 4H, $OC\underline{H}_2NH$). ^{13}C NMR (D_2O): δ = 159.3 (1C, $\underline{C}$=O); 64.2 (2C, $\underline{C}H_2$). ^{15}N NMR (H_2O): $\delta_{CD_3NO_2}$ = −280.5 ($OCH_2\underline{N}H$). Melting point: 114 °C.

1-Ureidomethyl urea (MDU)

1-Ureidomethyl urea was prepared from both industrial and ^{15}N-labeled urea following Murray's approach.[95] The yield was 65% with regard to formaldehyde at 95% purity at 50-g scale. Labeled material was prepared at 0.5-g scale with a yield of 30%.

TLC: R_f = 0.30 (blue spot); ^{1}H NMR (H_2O): δ = 6.8 (bt, J = 6.3 Hz, 2H, $N\underline{H}CH_2N\underline{H}$); 5.8 (s, 4H, $N\underline{H}_2$); 4.43 (t, J = 6.3 Hz, 4H, $NHC\underline{H}_2NH$). ^{13}C NMR (H_2O): δ = 161.2 (2C, $\underline{C}$=O); 46.4 (1C, $NH\underline{C}H_2NH$). ^{15}N NMR (H_2O): $\delta_{CD_3NO_2}$ = −286 (d, $^{1}J_{N,H}$ = |90| Hz, 2N, $\underline{N}HCH_2\underline{N}H$); −303 (t, $^{1}J_{N,H}$ =|86| Hz, 2N, $\underline{N}H_2$). Melting point: 201 °C (decomposition).

1-Hydroxymethyl-3-(3-hydroxymethylureidomethyl) urea (bishydroxymethyl-MDUs)

To a solution of 3 g of 1-ureidomethylurea in 100 ml of water, an aqueous solution of formaldehyde ($x_{0,FA}$ = 0.3g/g) was slowly added at 60 °C. Both solutions were previously adjusted to a pH value of 9.0. The mixture was stirred for 20 min. The precipitate was filtered off, washed twice with water, washed once with diethyl ether, and dried under vacuum. The precipitate was identified as consisting largely of 1-hydroxymethy-3-(3-hydroxymethylureidomethyl) urea by NMR spectroscopy. The yield was 31.6% with regard to 1-ureidomethyl urea.
TLC: R_f = 0.21 (green spot); ^{1}H NMR (H_2O): δ = 7.0 (2H, $N\underline{H}CH_2OH$); 6.8 (2H, $N\underline{H}CH_2N\underline{H}$); 4.8 (4H, $NHC\underline{H}_2OH$); 4.4 (2H, $NHC\underline{H}_2NH$). ^{13}C NMR (H_2O): δ = 159.5 (2C, $\underline{C}$=O); 64.2 (2C, $NH\underline{C}H_2OH$); 46 (1C, $NH\underline{C}H_2NH$). ^{15}N NMR (H_2O): $\delta_{CD_3NO_2}$ = −279 (2N, $\underline{N}HCH_2OH$); −286 (2N, $\underline{N}HCH_2\underline{N}H$).

1,3-Bismethoxymethyl urea

1,3-Bismethoxymethyl urea was obtained following Kadowaki's approach[4] with a yield of 35.6% at 99% purity.

TLC: R_f = 0.70 (yellow spot); ^{1}H NMR (H_2O): δ = 7.3 (bt, J = 6.8 Hz, 2H, $CH_3OCH_2N\underline{H}$); 4.58 (d, J = 6.8 Hz, 4H, $CH_3OC\underline{H}_2NH$); 3.29 (s, 6H, $C\underline{H}_3OCH_2NH$). ^{13}C NMR (H_2O): δ = 159.5 (1C, $\underline{C}$=O); 72.1 (2C, $CH_3O\underline{C}H_2NH$); 54.4 (2C, $\underline{C}H_3OCH_2NH$). ^{15}N NMR (H_2O): $\delta_{CD_3NO_2}$ = −286.8 (d, $^{1}J_{N,H}$ = |91.6| Hz, $CH_3OCH_2\underline{N}H$). MS (EI): m/z = 133.1(M^+–CH_3); 117.1 (M^+–OCH_3); 101.1 (M^+–OCH_3–CH_3); 85.0 (M^+–2 OCH_3); 60.1 (M^+–2 CH_2OCH_3). Melting point: 96 °C.

3,5-Bismethoxymethyl-1,3,5-oxadiazinan-4-on (1,3-bismethoxymethyl uron)

Synthesis was carried out as reported by Kadowaki[4] and Paquin.[96] To 400 g aqueous formaldehyde solution ($x_{0,FA}$ = 0.3 g/g), 15 g $Ba(OH)_2$ and 60.1 g urea were added. The mixture was refluxed for 10 min while stirring. Then, it was reduced under vacuum until most of the water evaporated while keeping the temperature below 40 °C. The remaining viscous liquid was taken up with 1 l of methanol. After addition of 40 ml hydrochloric acid (x_m = 0.37 g/g), the mixture was stirred for 12 h at ambient temperature. After neutralization with $Ba(OH)_2$, the methanol was removed under vacuum. The residue was taken up with 0.5 l of chloroform and filtered to remove inorganic salts. The chloroform was evaporated. The residue was taken up with diethyl

ether. 1,3-Bismethoxymethyl urea was filtered off as precipitate. After removal of the solvents, the mother liquors were subjected to vacuum distillation. Three fractions were obtained between 110 and 115 °C at 1.5–1.7 mbar. The oily liquid was identified as 3,5-bismethoxymethyl-1,3,5-oxadiazinan-4-on by NMR spectroscopy. The yield was 4 g, representing 2% yield with regard to urea. The high yield reported by Kadowaki could not be reproduced here. The low selectivity of the uron formation may be explained by competition of the ring condensation with the formation of the methyl ether.

TLC: R_f = 0.79 (yellow spot); ^{1}H NMR (D_2O): δ = 5.03 (s, 4H, $NC\underline{H}_2OCH_3$); 4.78 (s, 4H, $NC\underline{H}_2OC\underline{H}_2N$); 3.34 (s, 6H, $OC\underline{H}_3$). ^{13}C NMR (D_2O): δ = 155.1 (1C, $\underline{C}$=O); 78.3 (2C, N $\underline{C}H_2OCH_3$); 75.6 (2C, $N\underline{C}H_2O\underline{C}H_2N$); 55.2 (2C, $O\underline{C}H_3$). ^{15}N NMR (H_2O): $\delta_{CD_3NO_2}$ = −280.0 ($\underline{N}CH_2OCH_2\underline{N}$). MS (EI): m/z = 190.1 (M^+); 175.1 (M^+–CH_3); 159.1 (M^+–OCH_3); 143.1 (M^+–CH_2OCH_3); 128.1 (M^+–$2OCH_3$); 114.1 (M^+–$2CH_2OCH_3$).

Mixture of 1,3,5-Oxadiazinan-4-ones

Following Beachem's[77] procedure, a solution of 1 g 3,5-bismethoxymethyl-1,3,5-oxadiazinan-4-on in 300 ml of water was refluxed with 2.95 g of dimedone (5,5-dimethylcyclohexane-1,3-dion) for 20 min. After cooling down to room temperature, the precipitate was removed by filtration. The mother liquors were reduced to approximately 10% of the original volume while maintaining the temperature below 50 °C and filtered again to remove all solids. The liquors were reduced to dryness and recrystallized from acetonitrile. The obtained crystals were identified as 1,3,5-oxadiazinan-4-on; the liquors contained a mixture of 3-hydroxymethyl-1,3,5-oxadiazinan-4-on and 3,5-bishydroxymethyl-1,3,5-oxadiazinan-4-on. No attempt was made to further separate the latter two components, as this two-component mixture was sufficient for characterization by NMR spectroscopy.

1,3,5-Oxadiazinan-4-on, uron

Prepared as described earlier.

TLC: R_f = 0.46 (yellow spot). ^{1}H NMR (D_2O): δ = 7 (s, 2H, $N\underline{H}CH_2OCH_2N\underline{H}$); 4.86 (s, 4H, $NHC\underline{H}_2OC\underline{H}_2NH$). ^{13}C NMR ($D_2O$): δ = 156.5 (1C, $\underline{C}$=O); 74.1 (2C, $NH\underline{C}H_2O\underline{C}H_2NH$).

3-Hydroxymethyl-1,3,5-oxadiazinan-4-on, hydroxymethyl uron

Prepared as described earlier.

^{1}H NMR (D_2O): δ = 7 (s, 1H, $HOCH_2NCH_2OCH_2N\underline{H}$); 4.99 (s, 2H, $HOCH_2NC\underline{H}_2OCH_2NH$); 4.88 (s, 2H, $HOCH_2NCH_2OC\underline{H}_2NH$); 4.81 (s, 2H, $HOC\underline{H}_2NCH_2OCH_2NH$). ^{13}C NMR ($D_2O$): δ = 155.5 (1C, $\underline{C}$=O); 77.7 (1C, $HOCH_2N\underline{C}H_2OCH_2NH$); 74.6 (1C, $HOCH_2NCH_2O\underline{C}H_2NH$); 67.3 (1C, $HO\underline{C}H_2NCH_2OCH_2NH$).

3,5-Bis-hydroxymethyl-1,3,5-oxadiazinan-4-on, bishydroxymethyl uron

Prepared as described earlier.

^{1}H NMR (D_2O): δ = 5.02 (s, 4H, $HOCH_2NC\underline{H}_2OC\underline{H}_2NCH_2OH$); 4.84 (s, 4H, $HOC\underline{H}_2NCH_2OCH_2NC\underline{H}_2OH$). ^{13}C NMR ($D_2O$): δ = 154.8 (1C, $\underline{C}$=O); 78.2 (2C, $HOCH_2N\underline{C}H_2O\underline{C}H_2NCH_2OH$); 67.7 (2C, $HO\underline{C}H_2NCH_2OCH_2N\underline{C}H_2OH$).

Supporting Information

Additional supporting information may be found in the online version of this article at the publisher's website.